



# DAFNE

A **D**ecision-**A**lytic **F**ramework to explore the  
water-energy-food **N**exus in complex and transboundary  
water resources systems of fast growing developing countries

## INTEGRATED MODEL OF THE WEF NEXUS

Deliverable D3.5

November 2019



**Programme Call:** ..... Water-5-2014/2015

**Project Number:** ..... 690268

**Project Title:** ..... DAFNE

**Work-Package:** ..... WP3

**Deliverable #:** ..... D3.5

**Deliverable Type:** ..... Document

**Contractual Date of Delivery:** 31 August 2019

**Actual Date of Delivery:** ..... 30 November 2019

**Title of Document:** ..... Integrated model of the WEF nexus

**Author(s):** ..... Leading Author: HWRM-ETHZ

..... Contributions from EM-ETHZ, AC-ETHZ, POLIMI, KU Leuven,  
VISTA-GEO, EIPCM

**Availability:** ..... This report is public.

<b>Document revisions</b>		
<i>Author</i>	<i>Revision content</i>	<i>Date</i>
Scott Sinclair	First draft table of contents	2019/08/08
Fritz Kleinschroth	Draft ecosystem services	2019/09/26
Scott Sinclair	Comment ecosystem services	2019/10/03
Ksenia Koroleva, Darien Miranda, Marco Micotti, Scott Sinclair	Discussions evaluation indicators – structure for sharing between tools	2019/09/23- 2019/10/29
Fritz Kleinschroth	Update ecosystem services	2019/10/31
Fritz Kleinschroth	Revision ecosystem services	2019/11/14
Giulia Battista	OTB sediment simulation results	2019/11/15
Rob Hillen, Matteo Giuliani, Marco Micotti, Scott Sinclair	Email discussions AquaCrop coupling	2019/09/10 – 2019/11/19
Elisa Calamita	Figures – GLM coupling	2019/11/26
Scott Sinclair	Updated draft – all sections	2019/11/28
Paolo Burlando	Final review	2019/11/29
Paolo Bulando	Submission	2019/11/30

## Table of Contents

<b>Integrated model of the WEF nexus.....</b>	<b>i</b>
<b>1. Introduction .....</b>	<b>1</b>
<b>2. Evaluation indicators identified in stakeholder engagement process.....</b>	<b>2</b>
2.1 Omo-Turkana basins .....	2
2.2 Zambezi river basin .....	5
<b>3. Description of integrated WEF model .....</b>	<b>7</b>
3.1 Linkages Between the DAF and the WEF .....	8
3.2 TOPKAPI-ETH Integrated Components .....	9
3.3 Linking TOPKAPI-ETH and AquaCrop .....	9
3.3.1 Simulation of AquaCrop under the DAF optimal policies .....	10
3.4 Linking TOPKAPI-ETH and the General Lake Model .....	14
3.4.1 Input for GLM .....	14
3.4.2 Output from GLM .....	14
3.5 Integration of Additional WEF Sub-Models .....	15
3.5.1 Ecosystem services models .....	16
<b>4. Subset of indicators computable with WEF model components .....</b>	<b>27</b>
4.1 Omo-Turkana basins .....	27
4.2 Zambezi river basin .....	29
<b>5. Conclusions .....</b>	<b>30</b>
<b>6. References .....</b>	<b>31</b>
<b>Appendix – OTB sediment modelling results .....</b>	<b>33</b>

## List of Tables

Table 1 – OTB Energy indicators from stakeholder engagement.....	2
Table 2 – OTB Food indicators from stakeholder engagement .....	2
Table 3 – OTB Water and Ecosystem indicators from stakeholder engagement .....	3
Table 4 – OTB Socio-economic indicators from stakeholder engagement.....	4
Table 5 – ZRB Energy indicators from stakeholder engagement .....	5
Table 6 – ZRB Food indicators from stakeholder engagement .....	5
Table 7 – ZRB Water and Ecosystem indicators from stakeholder engagement .....	6
Table 8 – ZRB Socio-economic indicators from stakeholder engagement.....	7
Table 9 – Area (ha) of flood recession agriculture in the Dassanech woreda reported by different sources .....	25
Table 10 – OTB Energy indicators to be computed by the WEF model .....	27
Table 11 – OTB Food indicators to be computed by the WEF model .....	27
Table 12 – OTB Water and Ecosystem indicators to be computed by the WEF model .....	28
Table 13 – OTB Socio-economic indicators to be computed by the WEF model .....	28
Table 14 – ZRB Energy indicators to be computed by the WEF model .....	29
Table 15 – ZRB Food indicators to be computed by the WEF model.....	29
Table 16 – ZRB Water and Ecosystem indicators to be computed by the WEF model.....	30
Table 17 – ZRB Socio-economic indicators to be computed by the WEF model .....	30



## List of Figures

Figure 1 – Overview sketch of the DAFNE stakeholder participatory process and modelling framework. ....	1
Figure 2 – Concept sketch of integrated WEF model structure. Including currently available sub-models. ....	8
Figure 3 – AquaCrop simulation procedure (adapted from Vanuytrecht et al., 2014). The inputs variables of rainfall, reference crop evapotranspiration ( $ET_0$ ; Allen et al., 1998) and air temperature circled in blue are obtained from the AWE-GEN-2d simulations. The irrigation allocation (ringed in green), is obtained from the TOPKAPI simulations using the DAF optimal operating policy associated with a given pathway. ....	10
Figure 4 – The system model configuration for the OTB. A matching spatially detailed configuration is set up for TOPKAPI-ETH, to compute the time-series of water allocations required by AquaCrop to compute the relevant evaluation indicators for the Kuraz and private agriculture irrigation districts. An irrigation efficiency of 60% has been assumed on the basis of literature studies. ....	11
Figure 5 – Ten main climate zones in OTB and corresponding locations for which crop yield was modelled for D2.2. ....	12
Figure 6 – Operational and planned irrigation schemes identified in the OTB. The dot size reflects the scheme size. ....	12
Figure 7 – The system model configuration for the ZRB. A set of matching spatially detailed configurations is set up for TOPKAPI-ETH, to compute the time-series of water allocations required by AquaCrop to compute the relevant evaluation indicators for the 8 irrigation districts (green rectangles). ....	13
Figure 8 – Ten main climate zones in ZRB and corresponding locations for which crop yield was modelled for D2.2. ....	13
Figure 9 – Operational and planned irrigation schemes identified in the ZRB. The dot size reflects the scheme size. ....	14
Figure 10 – Flow chart showing the link between the weather generator, DAF (through the hydrological model TOPKAPI), and GLM to produce the water quality indicators related to water temperature and dissolved oxygen. ....	15
Figure 11 – Validation of the GLM computed water temperature and dissolved oxygen concentration for lake Kariba (Calamita et al., 2019). ....	15
Figure 12 – Water levels at 11 locations along the Omo river and in Lake Turkana measured by remote sensing (Schwatke <i>et al</i> 2015). The length of time series varies depending on the availability of suitable imagery. ....	17
Figure 13 – Annual water level variation (difference between min and max observed values) for A) Omo river at location 7 in Fig. 1 and B) Lake Turkana (data for 2019 until October). ....	18
Figure 14 – Lake shore variations in two-month intervals between 2010 and 2019 showing the seasonal variation before and after the construction of Gibe III dam. Inset A) shows overall lake levels, B) the extent of the northern end of the lake near the delta as depicted above and C) in Fergusson's Gulf. ....	18
Figure 15 – Length of the river channels within the Omo delta from 1972 to 2019. Left: Year of first appearance, right: total length. ....	20
Figure 16 – Leaf Area Index (LAI) inside annually flooded areas of the Omo Delta and their size. ....	21
Figure 17 – Unsupervised vegetation classification for the Omo delta based on LAI time series derived from Landsat and Sentinel 2 imagery. Shown are six classes with their respective LAI time series. Linear regression lines are added to aid visual interpretation. White areas of the	

map are not classified due to generally low vegetation signal from inundation or they are part of the desert.....	22
Figure 18 – Leaf area index variation within buffers in 100 m increments around the lower Omo River based on Sentinel 2 imagery. Top: development over time, bottom: average across years. Data by VISTA remote sensing. ....	23
Figure 19 – Difference in Leaf Area Index (LAI) between Landsat 8 and Sentinel 2 images taken in the dry and the wet season. Pink areas show higher values in the wet season, green areas higher values in the dry season due to irrigation (lower part of the image) and ground water provided by the river. ....	24
Figure 20 – Relationship between observed flood recession agriculture area and modelled discharge in the lower Omo (data provided by F. Semeria, POLIMI). ....	25
Figure 21 – Field-based account of ongoing flood-recession agriculture (March 2019, only the western branch of the river in the delta was covered) compared to abandoned areas that were detected with active cultivation on high resolution imagery from 2011.....	26

## Abbreviations

DAF	Decision Analytic Framework model
NSL	Negotiation Simulation Lab
OTB	Omo-Turkana basins
WEF	Integrated Water, Energy and Food model
ZRB	Zambezi river basin



# 1. INTRODUCTION

The main objective of this report is to provide a description of the integrated Water, Energy and Food (WEF) model in the context of the DAFNE framework for analysing and evaluating the nexus. Figure 1 provides an overview sketch of the DAFNE stakeholder participatory process and modelling framework.

Through a stakeholder engagement process during and following the first Negotiation Simulation Labs (NSL) in each of the study basins, a detailed inventory of Issues, Actions and Indicators was compiled. Issues are a description of both beneficial and harmful activities taking place in the basins, in relation to the use of water. Actions are the planned and potential future interventions which might impact the shared use of the water resource across the various sectors (in either beneficial, or negative ways). A combination of actions, and the timing of their implementation, constitutes a potential development pathway. Finally, Indicators are a set of evaluation metrics that can be used to rank the value of a set of pathways in terms of their benefit to a given water use sector (e.g. Agriculture, Hydropower etc.).

The Decision Analytic Framework (DAF) is used to select a subset of efficient pathways (and an optimal system operation policy) from the universe of possible pathways constructed by varying the timing and sequencing of actions in the basin. Because this optimization step is computationally demanding, a simplified system model is used, and the ranking of pathways is based on a subset of strategic design indicators taken from the full list of indicators.

The purpose of the WEF model, is to evaluate in detail the full set of indicators in a spatially distributed manner. To do this, the WEF has at its core a spatially distributed hydrological model that accounts for both the hydrological fluxes and anthropogenic activities in the basin. The hydrological model is linked with various complimentary models to allow the computation of evaluation indicators that are not directly obtained from the outputs of the hydrological model.

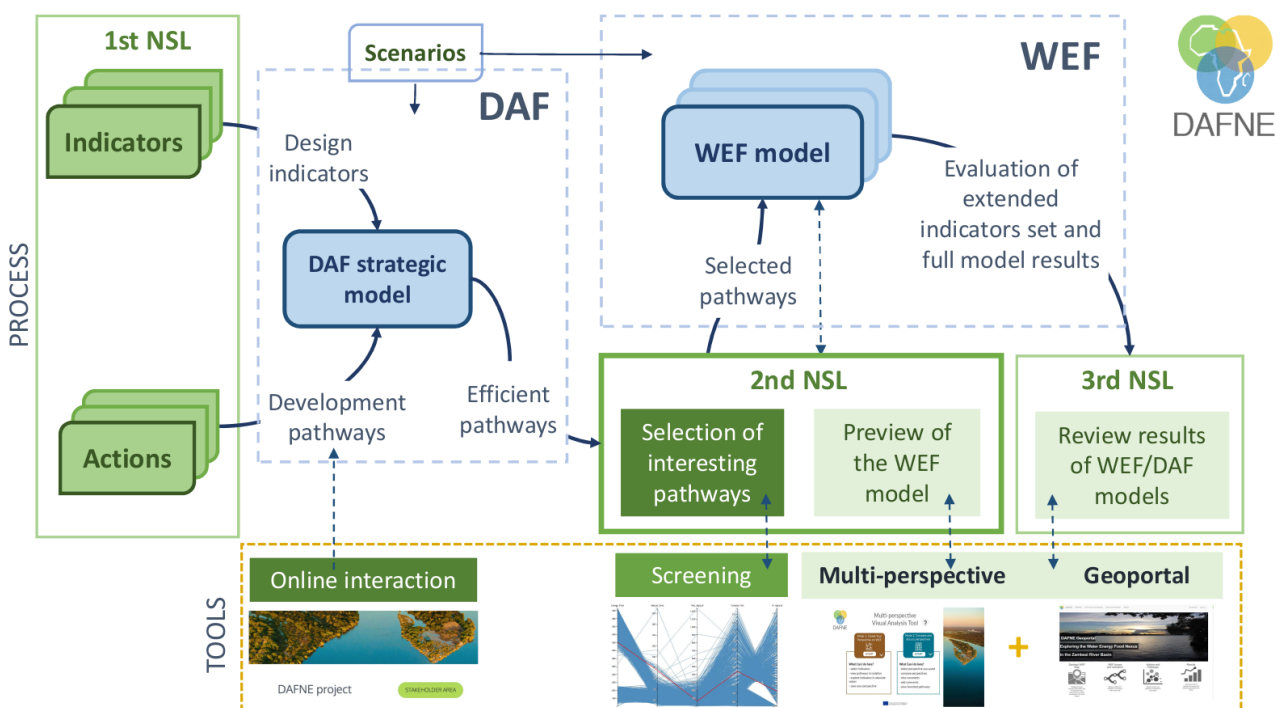


Figure 1 – Overview sketch of the DAFNE stakeholder participatory process and modelling framework.

In this report we inventory the evaluation indicators identified in the early stakeholder engagement activities (section 2). Then in section 3 we describe the components of the WEF as it is being implemented in the project, followed by a summary of the evaluation indicators that should be computed given the models that form the WEF (section 4). Finally, we present some concluding remarks in section 5.

## 2. EVALUATION INDICATORS IDENTIFIED IN STAKEHOLDER ENGAGEMENT PROCESS

In this section we present the indicator tables compiled as a result of the stakeholder engagement process during and after the first NSL meetings. The list is a result of combined input from the stakeholders and DAFNE partners.

It will become apparent in section 3, that this full list of indicators cannot be computed using the WEF model components available. In some cases, this is due to the lack of a suitable model formulation, but more commonly this is because there is no clear and direct link between the core model outputs and the indicators. Where it is not possible to compute an indicator, we drop it from the tables, and present the subset of WEF indicators in a similar set of tables in section 4.

The set of identified indicators are similar but not identical between the two case study basins. Therefore, a separate set of tables is presented for the Omo-Turkana basins (OTB) and Zambezi basin (ZRB) in sections 2.1 and 0 respectively.

### 2.1 OMO-TURKANA BASINS

Tables 1 through 4 present the indicators identified for the OTB for each of the four major water use sectors (Energy, Food, Water and Ecosystem services, and Socio-economic).

Table 1 – OTB Energy indicators from stakeholder engagement

ID	Short description	Definition
i_E_1	Energy production from hydro-power	Annual mean energy production in the Omo basin over the time horizon
i_E_2	Energy production from each power plant	Annual mean energy production for each power plant over the time horizon
i_E_3	Deficit with respect to energy demand	Annual mean energy deficit for each country in the Omo-Turkana basin over the time horizon
i_E_4	Lifespan of the dam	

Table 2 – OTB Food indicators from stakeholder engagement

ID	Short description	Definition
i_F_1	Agricultural Area	Area under crop cultivation, (per main crop) pasture and share of rivers/reservoirs used for fisheries or aquaculture
i_F_2	Yield of rainfed crops in terms of tons/ ha	Amount of crop produced per ha under current and future conditions
i_F_3	Yield of irrigated crops in terms of tons/ha	Amount of crop produced per ha under current and future conditions
i_F_4	Yield of rainfed and irrigated crops in terms of proteins/ ha	Amount of proteins produced per ha under current and future conditions
i_F_5	Yield of rainfed and irrigated crops in terms of calories/ ha	Amount of calories produced per ha or site or basin under current and future conditions

(Table 2 continued)

i_F_6	Water productivity of rainfed crops	Amount of water used to produce a unit of crop
i_F_7	Water productivity of irrigated crops	Amount of water used to produce a unit of crop
i_F_8	Irrigation water required for optimal production of irrigated crops	
i_F_9	Total livestock count	LSU/ha of utilised pasture area
i_F_10	Water required for optimal livestock production	Expressed as water demand per LSU / number of LSU. Including feed production and watering
i_F_11	Calorie yield from livestock	Expressed as total output including meat, milk (and blood) minus estimated losses.
i_F_12	Protein yield from livestock	Expressed as total output including meat and milk minus estimated losses.
i_F_13	Total fish catch and production	tons of fish produced or caught on a per hectare basis
i_F_14	Calorie yield from fish catch and production	Output in terms of calories, all species combined, losses considered as in (biomass(kg) * calories/kg) -losses (kg) per hectare
i_F_15	Protein yield from fish catch and production	Output in terms of proteins, all species combined, losses considered as in (biomass(kg) * calories/kg) -losses (kg) per hectare
i_F_16	Dietary supply adequacy - calories from crops, livestock and fisheries	Key indicator to estimate if food targets are being met . Formula: (calories produced in spatial unit/ population count) * calorie demand per capita
i_F_17	Dietary supply adequacy - proteins from crop, livestock and fisheries	Key indicator to estimate if food targets are being met . Formula: (proteins produced in spatial unit/ population count) * protein demand per capita

Table 3 – OTB Water and Ecosystem indicators from stakeholder engagement

ID	Short description	Definition
i_W_Ec_1	Magnitude of flooding	Surface water dynamics
i_W_Ec_2	Duration of flooding	
i_W_Ec_3	Water requirements for Habitat and fish migration	Seasonal flow patterns needed to maintain habitats and connectivity for fish species
i_W_Ec_4	Sediment transport	Amount of sediment eroded, transported by rivers, trapped behind dams, deposited in floodplains
i_W_Ec_5	Lake levels: Indicator for long-term variability of climate and water use patterns	Average lake levels should not be permanently below 362.3 masl, otherwise Ferguson's gulf will permanently dry out, with negative effects on fish stocks (Gownaris 2017)
i_W_Ec_6	Land cover change	Indicator for changes in land-use and vegetation (e.g. deforestation)
i_W_Ec_7	River discharge: Amount of flow at different river cross-sections in the basin	Baseline discharge statistics at Gibe III location shown in the diagram below. Average discharge values 1964-2001 (Jan: 78; Feb: 71; Mar: 61; Apr: 86; May: 141; Jun: 336; Jul: 942; Aug: 1529; Sep: 1058; Oct: 584; Nov: 217; Dec: 117)
i_W_Ec_8	Index of Hydrological alteration	Alteration of the hydrological regime with respect to a given reference
i_W_Ec_9	Evaporation rate from water bodies	

(Table 3 continued)

i_W_Ec_10	Water table (surface and groundwater level)	
i_W_Ec_11	water temperature alterations	difference of temperature between the upstream and downstream water temperature in °C.
i_W_Ec_12	dissolved oxygen	difference of temperature between the upstream and downstream water temperature in °C.

Table 4 – OTB Socio-economic indicators from stakeholder engagement

ID	Short description	Definition
i_SE_1	Population	total number of people
i_SE_2	Population Density	people per sq. km of land area
i_SE_3	Population by gender	total number of males, total number of females
i_SE_4	Population by age	total number of people aged 0-14, total number of people aged 15-64, total number of people aged 65 and over
i_SE_5	Population growth rate	% annual rate of change in population
i_SE_6	Population growth rate - urban	% annual rate of change in population in urban areas
i_SE_7	population growth rate - rural	% annual rate of change in population in rural areas
i_SE_8	Life Expectancy	Average life expectancy
i_SE_9	Life Expectancy by gender	average life expectancy of males, average life expectancy of females
i_SE_10	Infant mortality	% deaths of infants under 1year per 1000 live births
i_SE_11	HDI Ranking	Ranking based on Human Development Index score
i_SE_12	Employment rate	% of population in employment
i_SE_13	Employment Per Sector	% of population employed in each sector
i_SE_14	Average household income	average income per household (in USD)
i_SE_15	Average household spend - Water	average monthly spend on Water per household
i_SE_16	Average household spend - Electricity	average monthly spend on Electricity per household
i_SE_17	Access to Electricity	% population with grid access
i_SE_18	Access to drinking water	% population with access to drinking water
i_SE_19	Access to sanitation	% population with access to sanitation facilities
i_SE_20	Population living in slums	% of urban population living in slums
i_SE_24	GDP	
i_SE_21	GDP per Capita	
i_SE_22	GDP per Sector*	
i_SE_23	GVA per Sector*	
i_SE_25	Gross Fixed Capital per Sector*	
i_SE_26	Water Price	
i_SE_27	Electricity Price	
i_SE_28	Displacement	Number of people who are forced to leave their homes (e.g., due to the construction of dams)
i_SE_29	Poverty	Poverty headcount ratio at \$1.90 a day (2011 PPP) (% of population)



(Table 4 continued)

i_SE_30	Accessibility of school education	Net enrolment rate, secondary, both sexes (%)
i_SE_31	Accessibility of medical facilities	Hospital beds (per 1000 people)

## 2.2 ZAMBEZI RIVER BASIN

Tables 5 through 8 present the indicators identified for the ZRB for each of the four major water use sectors (Energy, Food, Water and Ecosystem services, and Socio-economic).

Table 5 – ZRB Energy indicators from stakeholder engagement

ID	Short description	Definition
i_E_1	Energy production from hydro-power in river basin	The indicator measures yearly average performance in term of energy production from all the plants in the River Basin.
i_E_2	Energy production from hydro-power at national level	The indicator measures yearly average performance in term of energy production from all the plants of a given country.
i_E_3	Energy production from each hydro-power plant	The indicator measures yearly average performance in term of energy production of a given power plant
i_E_4	Deficit with respect to energy demand in the river basin	The indicator measures yearly average deficit with respect to the energy demand related to all the plants in the River Basin.
i_E_5	Deficit with respect to energy demand at national level	The indicator measures yearly average deficit with respect to the energy demand related to all the plants in a given country.
i_E_6	Deficit with respect to energy demand for each power plant	The indicator measures yearly average deficit with respect to the energy demand related to a given power plant

Table 6 – ZRB Food indicators from stakeholder engagement

ID	Short description	Definition
i_F_1	Agricultural Area	Area under crop cultivation, (per main crop) pasture and share of rivers/reservoirs used for fisheries or aquaculture
i_F_2	Yield of rain fed crops in terms of tons/ ha	Amount of crop produced per ha under current and future conditions
i_F_3	Yield of irrigated crops in terms of tons/ha	Amount of crop produced per ha under current and future conditions
i_F_4	Yield of rain fed and irrigated crops in terms of proteins/ ha	Amount of proteins produced per ha under current and future conditions
i_F_5	Yield of rain fed and irrigated crops in terms of calories/ ha	Amount of calories produced per ha or site or basin under current and future conditions
i_F_6	Water productivity of rain fed crops	Amount of water used to produce a unit of crop
i_F_7	Water productivity of irrigated crops	Amount of water used to produce a unit of crop

(Table 6 continued)

i_F_8	Irrigation water required for optimal production of irrigated crops	
i_F_9	Total livestock count	LSU/ha of utilised pasture area
i_F_10	Water required for optimal livestock production	Expressed as water demand per LSU / number of LSU. Including feed production and watering
i_F_11	Calorie yield from livestock	Expressed as total output including meat, milk (and blood) minus estimated losses.
i_F_12	Protein yield from livestock	Expressed as total output including meat and milk minus estimated losses.
i_F_13	Total fish catch and production	tons of fish produced or caught on a per hectare basis
i_F_14	Calorie yield from fish catch and production	Output in terms of calories, all species combined, losses considered as in (biomass(kg) * calories/kg) -losses (kg) per hectare
i_F_15	Protein yield from fish catch and production	Output in terms of proteins, all species combined, losses considered as in (biomass(kg) * calories/kg) -losses (kg) per hectare
i_F_16	Dietary supply adequacy - calories from crops, livestock and fisheries	Key indicator to estimate if food targets are being met . Formula: (calories produced in spatial unit/ population count) * calorie demand per capita
i_F_17	Dietary supply adequacy - proteins from crop, livestock and fisheries	Key indicator to estimate if food targets are being met . Formula: (proteins produced in spatial unit/ population count) * protein demand per capita

Table 7 – ZRB Water and Ecosystem indicators from stakeholder engagement

ID	Short description	Definition
i_W_Ec_1	Magnitude of flooding	Surface water dynamics
i_W_Ec_2	Duration of flooding	
i_W_Ec_3	Water requirements for Habitat and fish migration	Seasonal flow patterns needed to maintain habitats and connectivity for fish species
i_W_Ec_4	Sediment transport	Amount of sediment eroded, transported by rivers, trapped behind dams, deposited in floodplains
i_W_Ec_5	Land cover change	Indicator for changes in land-use and vegetation (e.g. deforestation)
i_W_Ec_6	River discharge: Amount of flow at different river cross-sections in the basin	
i_W_Ec_7	Index of Hydrological alteration	Alteration of the hydrological regime with respect to a given reference
i_W_Ec_8	Evaporation rate from water bodies	
i_W_Ec_9	Water table (surface and groundwater level)	
i_W_Ec_10	water temperature alterations	difference of temperature between the upstream and downstream water temperature in °C.
i_W_Ec_11	dissolved oxygen	difference of temperature between the upstream and downstream water temperature in °C.

Table 8 – ZRB Socio-economic indicators from stakeholder engagement

ID	Short description	Definition
i_SE_1	Population	total number of people
i_SE_2	Population Density	people per sq. km of land area
i_SE_3	Population by gender	total number of males, total number of females
i_SE_4	Population by age	total number of people aged 0-14, total number of people aged 15-64, total number of people aged 65 and over
i_SE_5	Population growth rate	% annual rate of change in population
i_SE_6	Population growth rate - urban	% annual rate of change in population in urban areas
i_SE_7	Population growth rate - rural	% annual rate of change in population in rural areas
i_SE_8	Life Expectancy	Average life expectancy
i_SE_9	Life Expectancy by gender	average life expectancy of males, average life expectancy of females
i_SE_10	Infant mortality	% deaths of infants under 1 year per 1000 live births
i_SE_11	HDI Ranking	Ranking based on Human Development Index score
i_SE_12	Employment rate	% of population in employment
i_SE_13	Employment Per Sector	% of population employed in each sector
i_SE_14	Average household income	average income per household (in USD)
i_SE_15	Average household spend - Water	average monthly spend on Water per household
i_SE_16	Average household spend - Electricity	average monthly spend on Electricity per household
i_SE_17	Access to Electricity	% population with grid access
i_SE_18	Access to drinking water	% population with access to drinking water
i_SE_19	Access to sanitation	% population with access to sanitation facilities
i_SE_20	Population living in slums	% of urban population living in slums
i_SE_24	GDP	
i_SE_21	GDP per Capita	
i_SE_22	GDP per Sector*	
i_SE_23	GVA per Sector*	
i_SE_25	Gross Fixed Capital per Sector*	
i_SE_26	Water Price	
i_SE_27	Electricity Price	
i_SE_28	Displacement	Number of people who are forced to leave their homes (e.g., due to the construction of dams)
i_SE_29	Poverty	Poverty headcount ratio at \$1.90 a day (2011 PPP) (% of population)
i_SE_30	Accessibility of school education	Net enrolment rate, secondary, both sexes (%)
i_SE_31	Accessibility of medical facilities	Hospital beds (per 1000 people)

### 3. DESCRIPTION OF INTEGRATED WEF MODEL

In this section we outline the structure of the integrated WEF model, including a description of the distributed hydrological model integrating natural and anthropogenic controls of the WEF nexus, and the primary linked models (AquaCrop and the General Lake Model). The general concept of

the WEF, is that it consists of an inter-linked suite of models that should be changed/refined when applying the modelling framework to a different basin which has different nexus issues. At the core is the spatially distributed hydrological model that simulates the main water fluxes in the basin, and operates hydropower releases and irrigation allocations according to the optimal policy produced from the DAF.

Figure 2 is a flow chart illustrating the concept. The strategic system model in the DAF is given a sequence of irrigation demands, and available flows upstream of the basin infrastructure. The outcome of the pathway, and operating policy optimization is to produce a set of efficient pathways, and the corresponding optimal system operation policies. The optimal policy aims to maximize hydropower energy production, and also minimize irrigation supply deficit. The hydrological model TOPKAPI-ETH (see deliverable D3.1) then performs detailed (in space and time) simulations of the basin water fluxes implementing the optimal policies. The hydropower releases according to the policy are fed into GLM for simulating water quality dynamics in the system reservoirs, and the irrigation allocations determined are fed into AquaCrop in order to compute crop yield and related food indicators. The same concept is applied to any model aimed to simulate additional direct and indirect components of the WEF, e.g. the additional sub-models for ecosystem services and socio-economic models. The final outcome of the simulations available from the WEF modelling framework is a spatially detailed set of evaluation indicators to aid decision makers in selecting between different development trajectories in the basin on the basis of the spatially and temporally impacts described by the indicators.

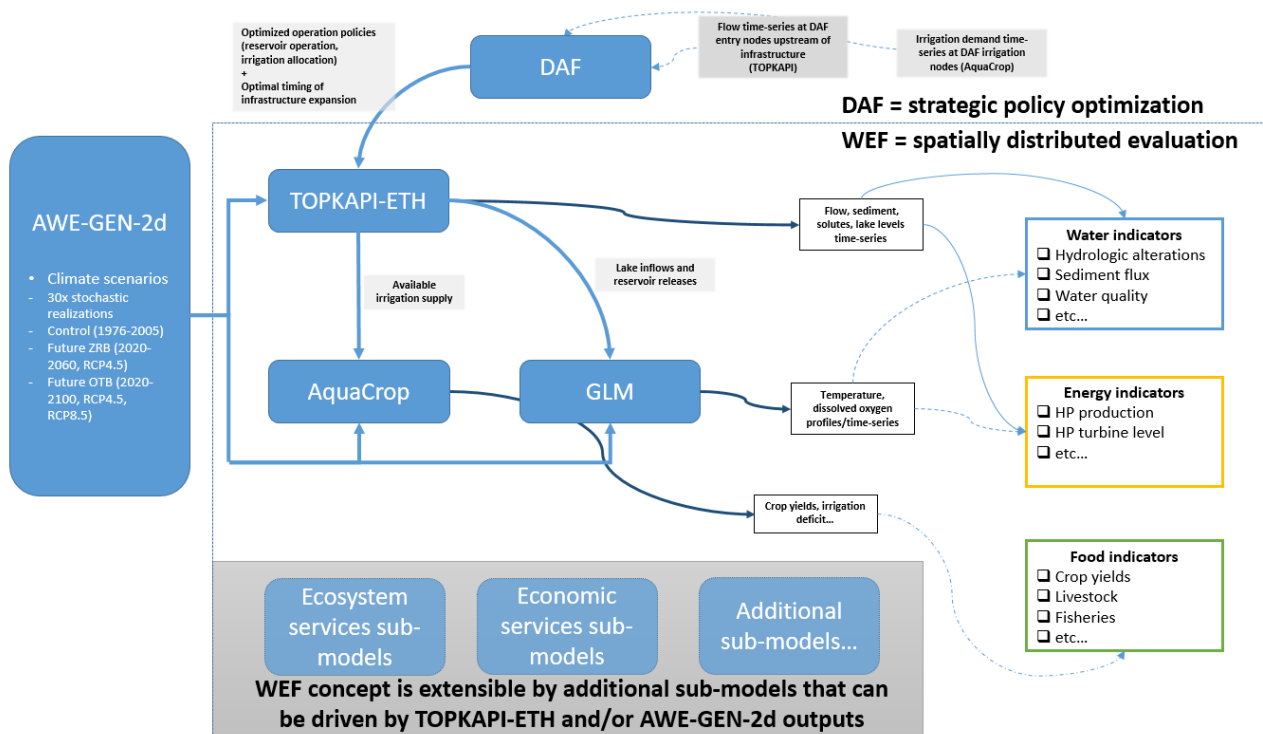


Figure 2 – Concept sketch of integrated WEF model structure. Including currently available sub-models.

### 3.1 LINKAGES BETWEEN THE DAF AND THE WEF

In deliverable D5.2 the architecture of the Decision Analytic Framework (DAF) for strategic optimization of the basin was described. The inputs to the DAF are streamflows at the nodes upstream of the basin infrastructure, and irrigation demands at the relevant agricultural district nodes in the case study basins. The output from the DAF is a fully coordinated operation policy for the basin hydropower releases and irrigation allocations, which depends on the state of the reservoirs in the

basin on a monthly scale. This policy is ingested into TOPKAPI, and used to allocate water for hydropower releases and irrigated agriculture. The policies form the link between the strategic DAF model, and the detailed WEF model of the basin system.

### 3.2 TOPKAPI-ETH INTEGRATED COMPONENTS

To reproduce the hydrologic response of the two river basins investigated we use a physically-explicit distributed hydrological model, which can simulate all the processes relevant to the space-time description of the water dynamics controlling streamflow, soil water content, evaporation and evapotranspiration on which the response of agriculture and ecosystems depend. In the subtask 3.1.1, the prototype model – TOPKAPI-ETH – developed by HWRM-ETHZ was recoded and further improved in some of its components in order to support the analysis of pathway evaluation indicators in detail over the entire river basin.

The main changes needed to support the DAFNE vision included:

- DAF operating policy integration
- Driving model by space-time high resolution climate scenarios
- Sediment transport<sup>1</sup>
- Conservative and non-conservative solute transport

The deliverable associated with the work done in the subtask is D3.1 “A distributed hydrological model to simulate hydrological response, transport processes and sediment dynamics” was delivered in M24. It provides a detailed description of the redesigned distributed hydrological model accounting for hydrologic transport processes and sediment dynamics in a spatially and temporally explicit fashion. The capabilities of the model are unique in that they allow modelling at high spatial and temporal resolution both the natural dynamics of the basin and the effects of the anthropic controls.

The model implementation required a significant effort, which is shortly summarised as follows:

- 70 000 lines of source code ground up
- 3 generations of TOPKAPI-ETH (TE) to coordinate
- Development time (TE64 > 8 years; TE2 approx. 3 years)
- Windows only → Windows and Linux same code base
- Structured for parallel computations

### 3.3 LINKING TOPKAPI-ETH AND AQUACROP

The purpose of this section is to outline the inter-linkage between the hydrological model TOPKAPI-ETH and the AquaCrop crop yield model, which will be used together in the DAFNE project, in order to compute food related evaluation indicators of the integrated Water, Energy, Food model (WEF). In Figure 2 the DAFNE modelling framework is outlined with a focus on the WEF components. In this section we describe how the optimal irrigation policies designed in the DAF inform AquaCrop’s irrigation allocations, through simulation of the basin system with TOPKAPI-ETH using the DAF optimized policies for operating the reservoirs and irrigation schemes.

FAO’s AquaCrop-model will be used to model the agricultural productivity of food, fodder and cash (coffee, tea, bio-energy) crops, and tested on trees as well as rangeland based on the data collected and geo-referenced in ST 2.1.3 both for rain-fed and irrigated conditions. It will also be used to predict site-specific agricultural productivity under the climate change scenarios (ST 2.3.1) for new irrigation schemes and in the projected extensions of the non-irrigated agricultural domain. For the irrigation schemes, optimal and minimal (deficit irrigation) water supply will be assessed. The design of the latter experiments will be coordinated with corresponding abstractions from the hydrological model.

<sup>1</sup> See the appendix for initial sediment modelling results on the Omo-Turkana basin

AquaCrop is a physically based crop water productivity model, that simulates crop development and production under various environmental conditions and management practices. The model has been calibrated for more than 30 different crops, including widely cultivated crops such as maize, wheat and sugarcane, as well as underutilized crops such as bambara groundnut and tef. As AquaCrop keeps an optimal balance between accuracy, robustness and simplicity, it only requires a limited number of easily obtainable input parameters. This makes the model applicable even in data-scarce conditions. AquaCrop has been applied multiple times to assess irrigation, crop and field management in African cropping systems. In the DAFNE context we plan to couple AquaCrop with the hydrological model used in ST 3.1.1, in order to take advantage of the spatially explicit simulation of soil water content resulting from lateral flow. This will allow the extrapolation of the AquaCrop results in the space domain by accounting for a more realistic representation of soil water dynamics due to the connectivity of surface and subsurface water fluxes.

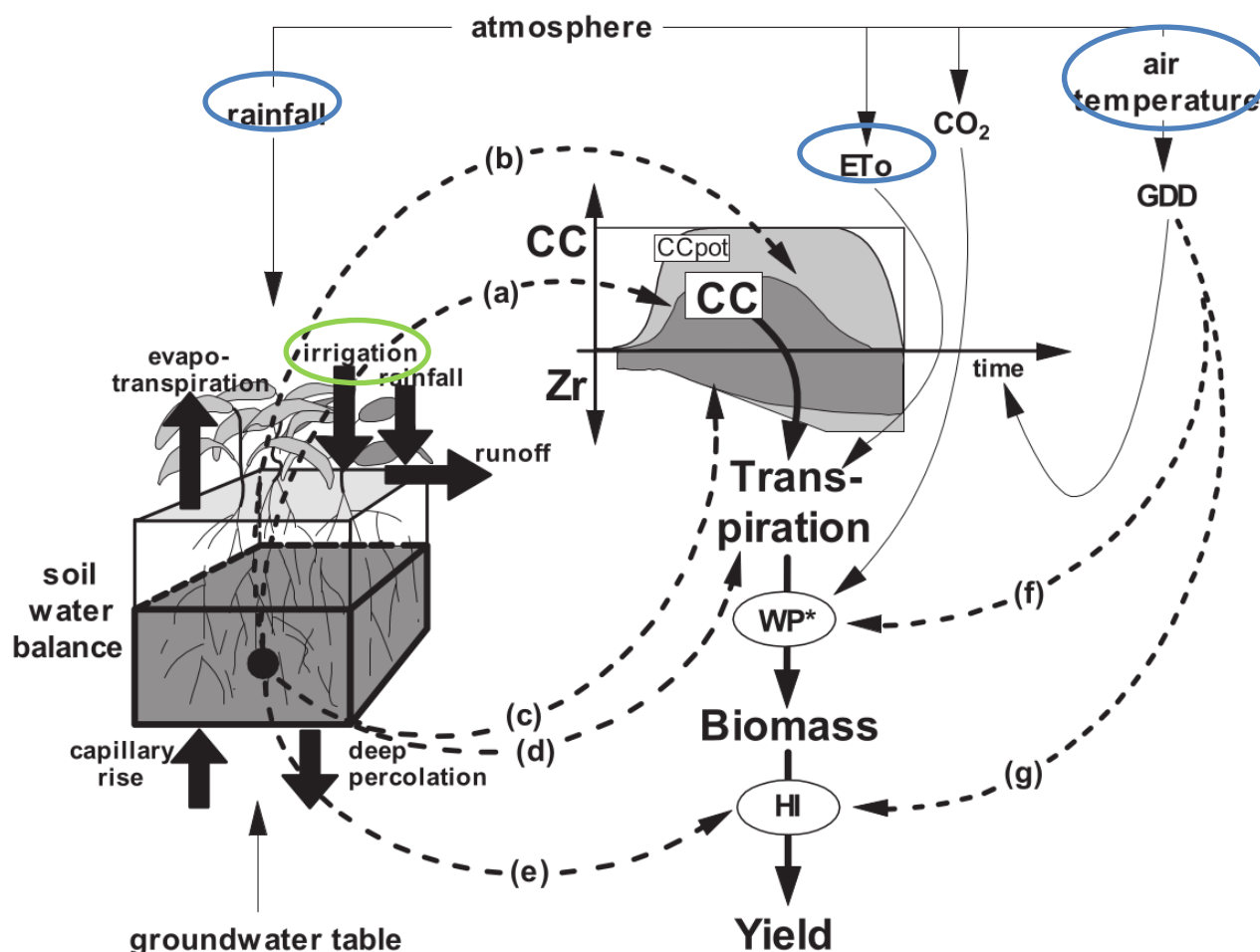


Figure 3 – AquaCrop simulation procedure (adapted from Vanuytrecht et al., 2014). The inputs variables of rainfall, reference crop evapotranspiration ( $ET_0$ ; Allen et al., 1998) and air temperature circled in blue are obtained from the AWE-GEN-2d simulations. The irrigation allocation (ringed in green), is obtained from the TOPKAPI simulations using the DAF optimal operating policy associated with a given pathway.

### 3.3.1 Simulation of AquaCrop under the DAF optimal policies

#### General concept for application in the case study basins

In general, the methodology is to run simulations of the case study catchments using TOPKAPI-ETH forced by the AWE-GEN-2d down-scaled climate trajectories, and with the infrastructure (reservoirs and irrigation abstractions) controlled by the relevant sub-set of operating policies identified from the DAF and screening process with basin stakeholders at the NSL meetings. This is illustrated in Figure 2.



Of relevance to the coupling with the AquaCrop WEF sub-model, TOPKAPI-ETH produces a time series of irrigation allocations for each irrigation district which is controlled by the DAF policy. AquaCrop simulations are run using the climate forcing realizations from AWE-GEN-2d, and Food indicators computed on the difference between present and future climates. In addition, (for the policy controlled irrigation districts), the irrigation allocations derived from the TOPKAPI-ETH simulations can be used to compute indicators against the optimal operation of the irrigation schemes (i.e. assuming all the required irrigation demand can be met, given a certain climate forcing).

The differences in the model configuration for each study basin are based on the final outputs of the DAF and NSL process. For the OTB the results from the DAF are for a single future basin configuration with multiple operation policies. While for the ZRB, the output of the DAF is the sequence and timing of constructing a set of new reservoirs, but with a single operations policy for each of the resulting basin configurations. The case study specifics are detailed in the sections below.

### Omo-Turkana basin

Figure 4 shows the system configuration to be modelled for the Omo-Turkana basins. Since the planned developments are already under way and relatively certain, the pathways in this case study are related to different policies of operating the system. Figure 5 shows the crop modelling done to inform the DAF for the strategic analysis, while Figure 6 illustrates to detailed layout of irrigation schemes to be modelled in the WEF.

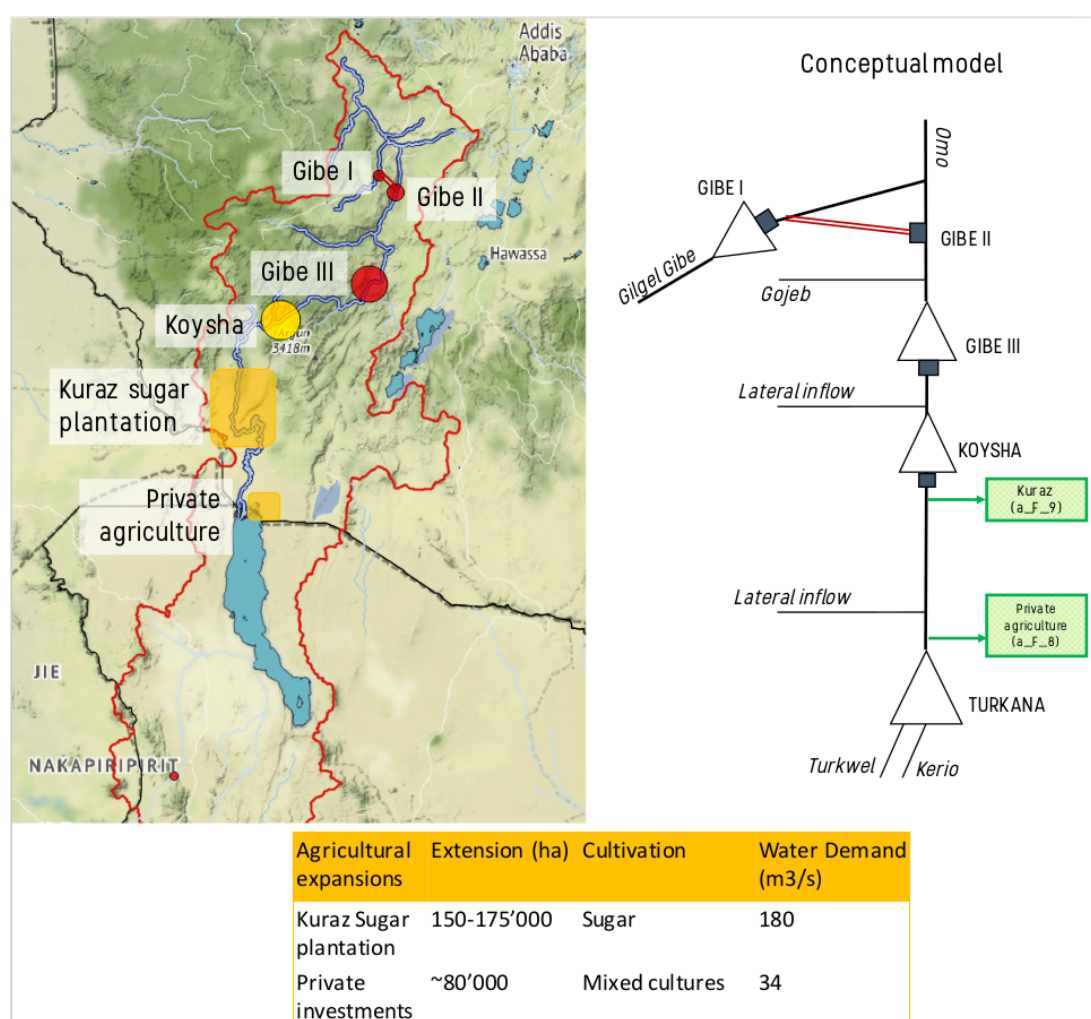


Figure 4 – The system model configuration for the OTB. A matching spatially detailed configuration is set up for TOPKAPI-ETH, to compute the time-series of water allocations required by AquaCrop to compute the relevant evaluation indicators for the Kuraz and private agriculture irrigation districts. An irrigation efficiency of 60% has been assumed on the basis of literature studies.

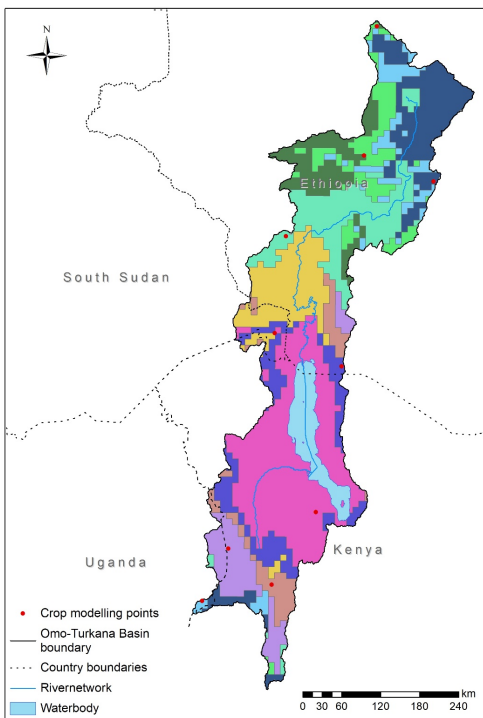


Figure 5 – Ten main climate zones in OTB and corresponding locations for which crop yield was modelled for D2.2.

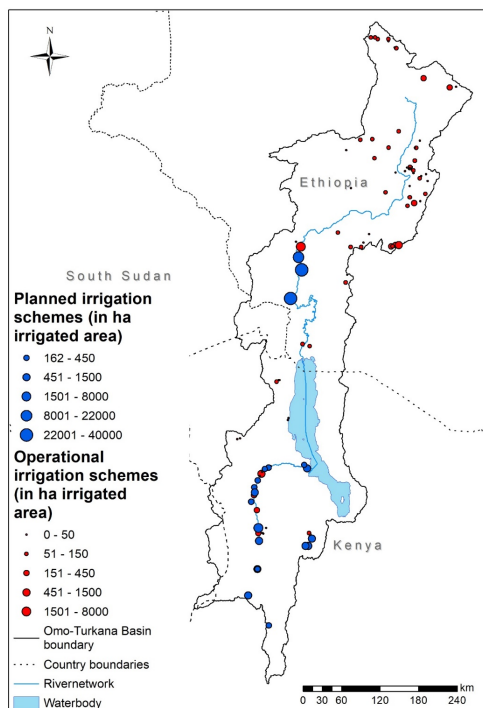


Figure 6 – Operational and planned irrigation schemes identified in the OTB. The dot size reflects the scheme size.

## Zambezi

For the Zambezi basin, the pathways to be modelled are determined according to the timing and sequencing of constructing the three planned hydropower reservoirs Batoka Gorge, Devils Gorge and Mphanda Nkuwa (see Figure 7). Figure 8 shows the crop modelling done to inform the DAF for



the strategic analysis, while Figure 9 illustrates to detailed layout of irrigation schemes to be modelled in the WEF.

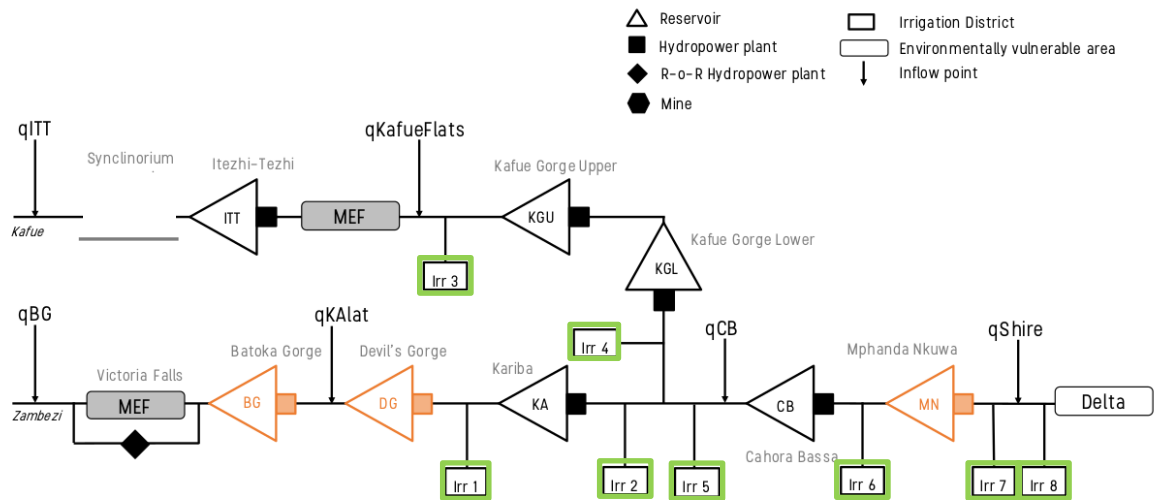


Figure 7 – The system model configuration for the ZRB. A set of matching spatially detailed configurations is set up for TOPKAPI-ETH, to compute the time-series of water allocations required by AquaCrop to compute the relevant evaluation indicators for the 8 irrigation districts (green rectangles).

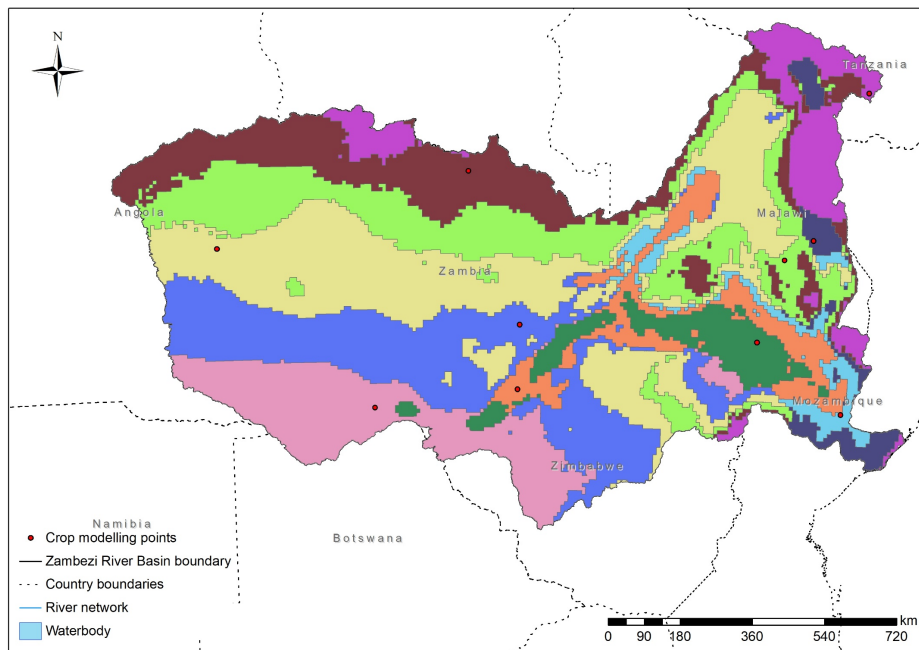


Figure 8 – Ten main climate zones in ZRB and corresponding locations for which crop yield was modelled for D2.2.

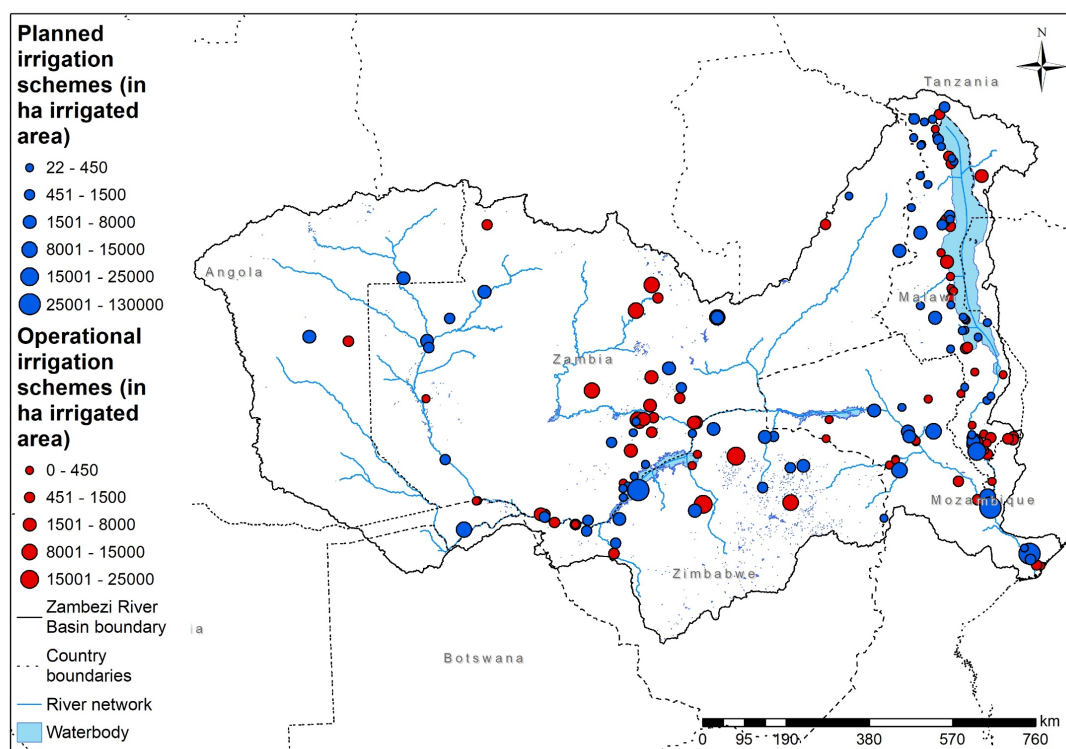


Figure 9 – Operational and planned irrigation schemes identified in the ZRB. The dot size reflects the scheme size.

### 3.4 LINKING TOPKAPI-ETH AND THE GENERAL LAKE MODEL

The coupling methodology that we will apply is to chain the hydrological model TOPKAPI and the lake/reservoir model GLM. The concept is to run the hydrological model to produce reservoir inflow and outflow time-series, which will be used to force the lake model in conjunction with identical meteorological forcing as used to drive the hydrological model. We also reuse the level-storage relationship for the reservoir in both models. The relevant water quality parameters (temperature and dissolved oxygen) as modified by the reservoir are thereafter expressed as water quality indicators downstream of the reservoir. Figure 10 shows the modelling process in the form of a flow chart. When calibration data are available (e.g. for lake Kariba), the GLM model is able to produce good results. Figure 11 shows validation results from a paper in preparation.

#### 3.4.1 Input for GLM

List of inputs required for GLM (with sources)

- Depth volume relationship
- Reservoir inflow time-series [TOPKAPI]
- Reservoir outflow time-series [TOPKAPI according to DAF policy]
- Precipitation forcing [AWE-GEN-2d]
- Temperature forcing [AWE-GEN-2d]
- Wind [AWE-GEN-2d]
- Cloud cover proportional [AWE-GEN-2d]
- Short wave rad/Long wave rad/Net radiation [AWE-GEN-2d]

#### 3.4.2 Output from GLM

- Temperature time-series downstream of the reservoir
- Dissolved oxygen concentration downstream of the reservoir

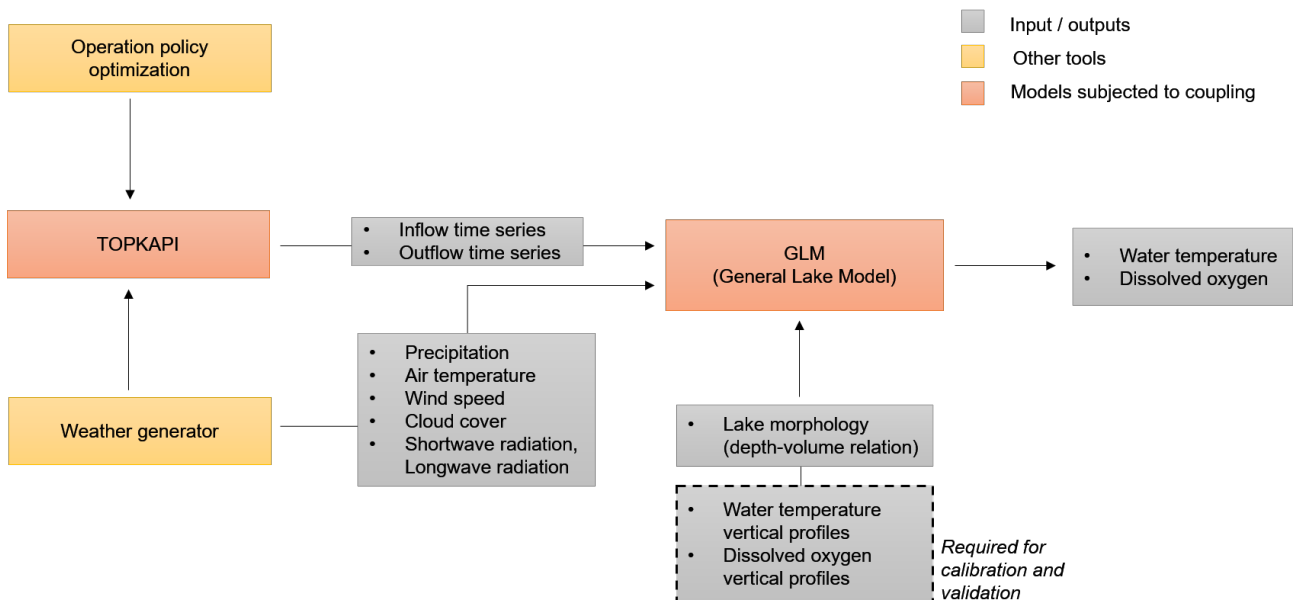


Figure 10 – Flow chart showing the link between the weather generator, DAF (through the hydrological model TOPKAPI), and GLM to produce the water quality indicators related to water temperature and dissolved oxygen.

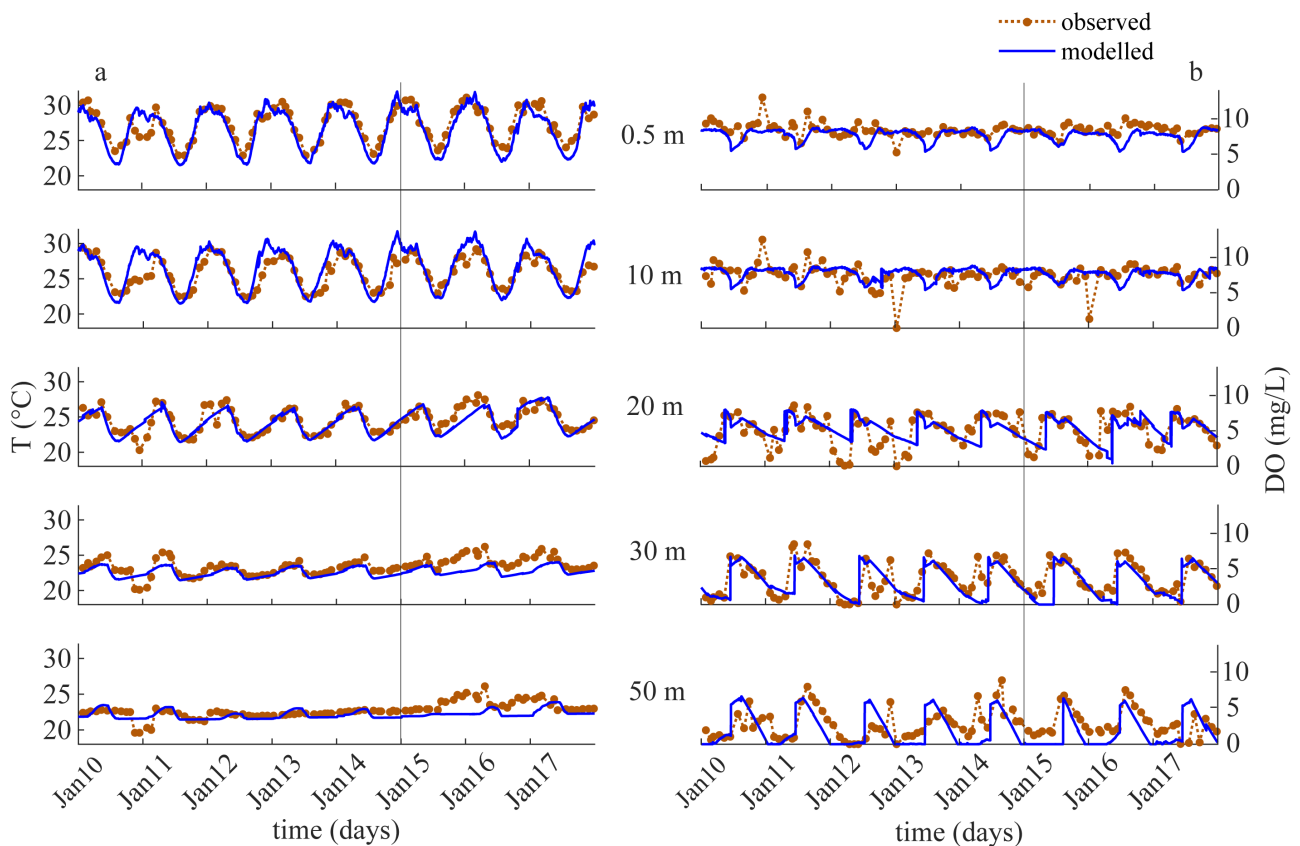


Figure 11 – Validation of the GLM computed water temperature and dissolved oxygen concentration for lake Kariba (Calamita et al., 2019).

### 3.5 INTEGRATION OF ADDITIONAL WEF SUB-MODELS

As no general ecosystem model exists and can be developed without a long-term effort to simulate impacts on a breadth of ecosystem components, we introduce in this section our thinking towards

producing concrete sub-models related to ecosystem services. The current discussion focuses on the Omo-Turkana basin, since the work is more advanced in this case study.

### 3.5.1 Ecosystem services models<sup>2,3</sup>

#### Linking ecosystems and ecosystem services with hydrological flows

Dam construction and irrigation agriculture along the Omo river have been associated with a reduction in seasonal flooding dynamics along the Omo and in the delta as well as with overall reduced water levels in Lake Turkana (Avery and Tebbs 2018, Gownaris *et al* 2017). The changes in natural dynamics put a serious threat on the following ecosystem services as summarized by Hodbod *et al.* (2019):

- Cultural ecosystem services (with implications for migration, conflicts and health): Spiritual interactions, sense of heritage, sense of place
- Provisioning ecosystem services (with implications for food security): Wild foods, pastoralism, flood retreat cultivation, fish breeding
- Regulating ecosystem services (underlying the cultural and provisioning services): Groundwater level, nutrient transfer, lake levels, flood protection

Different groups of peoples benefit differently from ecosystem services. Above-mentioned ecosystem services are particularly demanded by rural (often considered indigenous) communities that live as agro-pastoralists, pastoralists and fishers. Other people in the region, living as labor migrants, but also agro-industry investors and national governments and populations that live in other regions, demand ecosystem services based on the modification of river systems. This chapter focusses on indicators for ecosystem services demanded by people within the region and provided by free-flowing rivers.

As described in deliverable D3.4, to link hydrological flows with ecosystem services, the most useful change-indicators are inter- and intra-annual dynamics in lake and river levels, surface water extent, river morphology and resulting changes in riparian vegetation and extents of flood-recession agriculture. In the following sections, we describe the observed changes in each of these indicators, their importance for ecosystem services and their linkages with the hydrological system.

#### *Reduced seasonal variations in water levels and potential implications for fisheries*

Water levels are an indicator for hydrological dynamics that can be determined remotely with relatively low biases and variations. We obtained levels at 11 locations along the Omo river and Lake Turkana (Schwatke *et al* 2015). The estimations of river levels show differences in the magnitude of variability in water level at various locations since the construction and filling of Gibe III (Figure 12). While the levels in the newly created reservoir vary greatly, previously common seasonal oscillations in the downstream sections of the river have been reduced to almost zero at site 7. Site 10 is the only observation in the lowest part of the river and only the period from 2016 to 2019 is covered. Here, seasonal water level variations are still apparent. In combination with the modelled flow data, we will be able to “back-calculate” if these variations have been higher before. Levels of Lake Turkana fell during the filling period of Gibe III in 2015-2017, even more so as the filling period coincided with a climatically dry period. This effect is partially mitigated as since 2017 lake levels have risen again (Figure 14). However, the seasonal variation in flows of the Omo river have halved since 2015. This affected also the variability in Lake Turkana, where the three lowest seasonal variations since 2008 occurred after 2015. These changes have important implications for ecosystem services provided by riparian vegetation as we describe in the following sections and for fisheries as it has already been documented in the literature.

<sup>2</sup> Text and analyses: Fritz Kleinschroth

<sup>3</sup> Data: Fabian Niggemann, VISTA, Francesco Semeria, PoliMi, Christian Schwatke, TU Munich

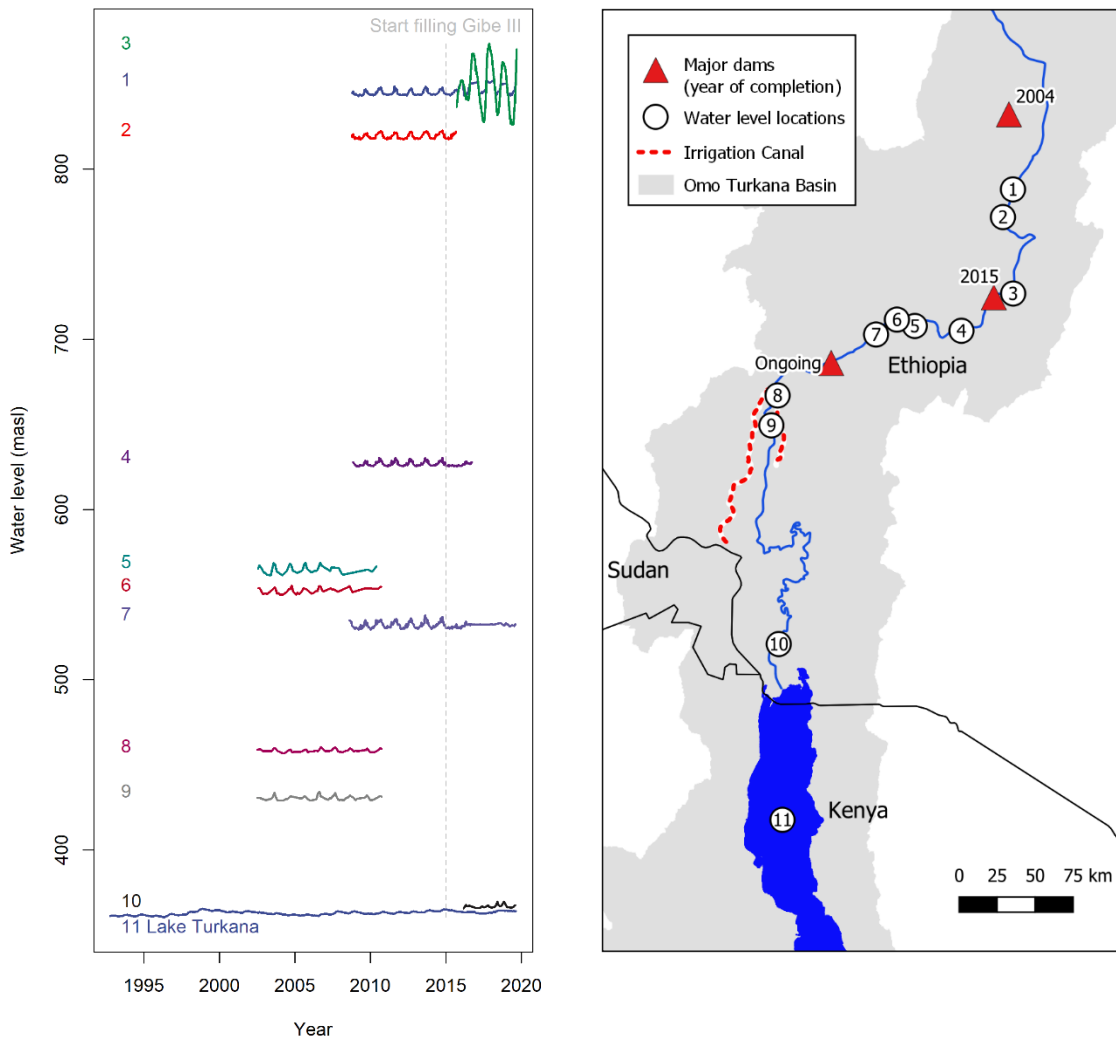


Figure 12 – Water levels at 11 locations along the Omo river and in Lake Turkana measured by remote sensing (Schwatke *et al* 2015). The length of time series varies depending on the availability of suitable imagery.

### Surface water extents of Lake Turkana

Our own model-based quantification of ecosystem dynamics is based on remotely sensed observations of the extent of Lake Turkana between 2010 and 2019. The overall levels and extent of Lake Turkana only decreased during the filling of Gibe III and showed an increasing trend since 2017. The extent of Fergusson's gulf, one of the most productive parts of Lake Turkana in terms of fish production, closely followed the trend of the overall lake levels. The lake area near the Omo delta, however, did not follow the strong decreasing trend after 2015 (Figure 14). This can be associated with an overall retraction of the delta area that we discuss below. In both the Omo Delta and at Fergusson's Gulf we find that the seasonal variation of the shoreline has diminished since the creation of Gibe III dam following the overall patterns in river flows (Figure 14).

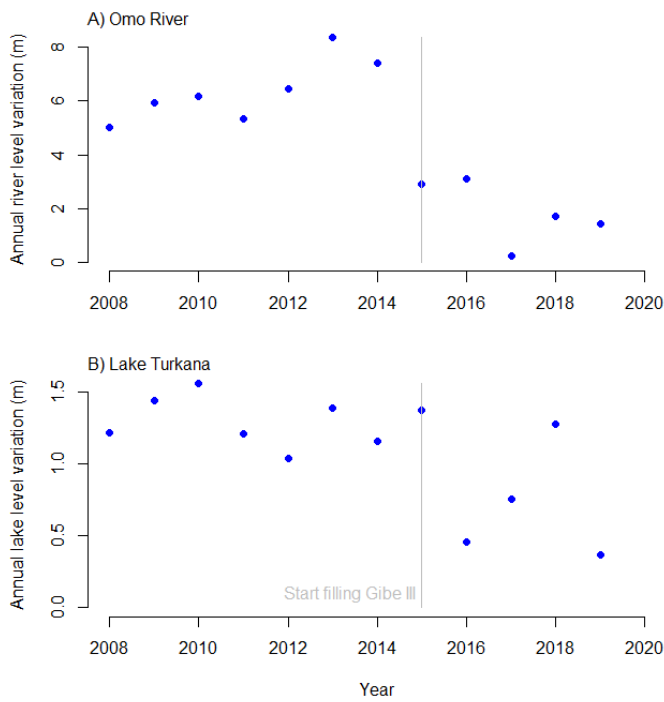


Figure 13 – Annual water level variation (difference between min and max observed values) for A) Omo river at location 7 in Fig. 1 and B) Lake Turkana (data for 2019 until October).

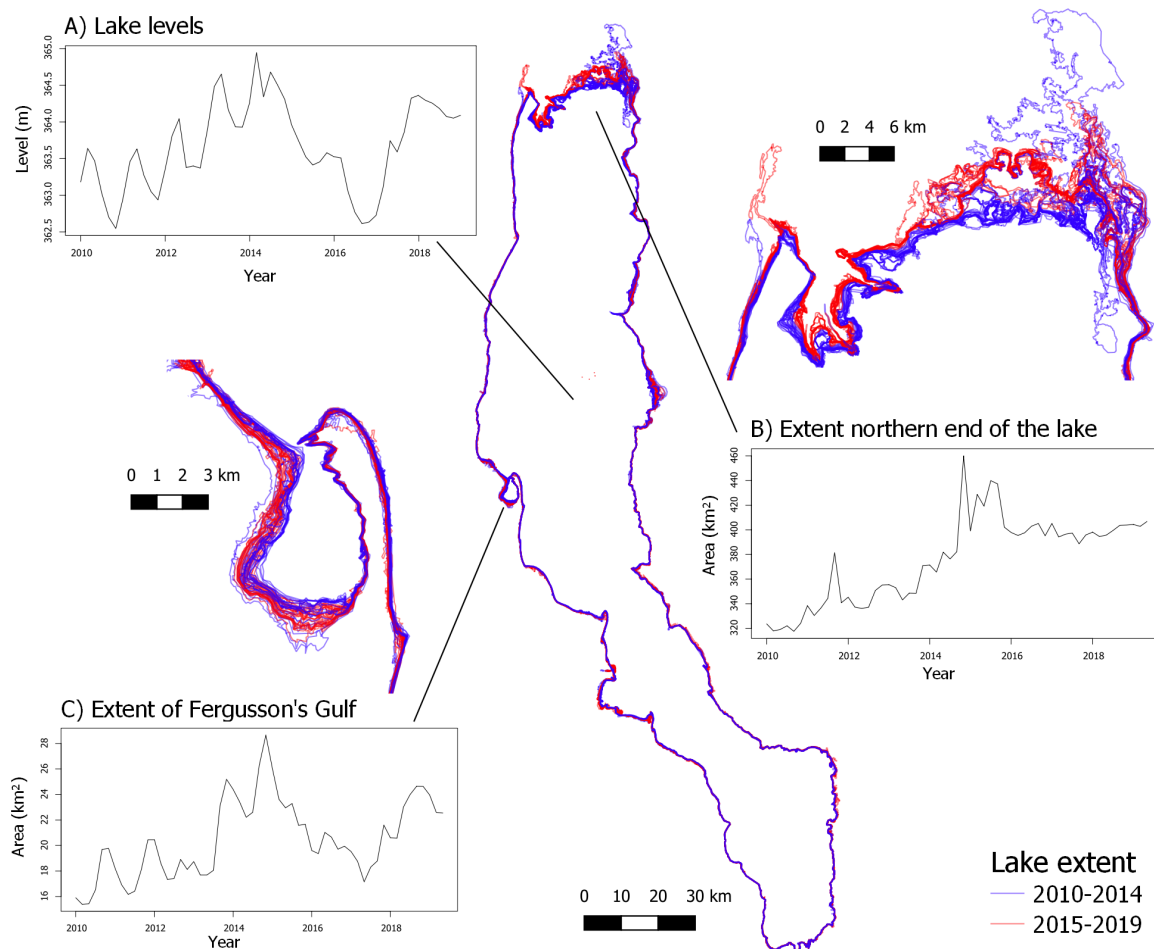


Figure 14 – Lake shore variations in two-month intervals between 2010 and 2019 showing the seasonal variation before and after the construction of Gibe III dam. Inset A) shows overall lake levels, B) the extent of the northern end of the lake near the delta as depicted above and C) in Fergusson's Gulf.

## Implications of lake levels and extent for fisheries

River systems with flood pulses are much more productive than river systems with static flows because they support floodplains as aquatic/terrestrial transition zones (ATTZ) that mobilize nutrients from land to water (Junk *et al* 1989). The same is true for lake systems: The magnitude of fluctuations in water levels are positively correlated with fish catch due to nutrient inputs and improved breeding habitats over seasonally flooded lands (Kolding and van Zwieten, 2012). The relative lake level fluctuation index (RLLF) is composed of the ratio between mean lake level amplitude and mean depth of a lake. The deep, stable Lake Tanganyika has a low seasonal RLLF of 0.13, whereas the shallower Lake Chad has a value of 30.28. Lake Turkana is somewhere in between, with a seasonal RLLF of 3.72 (Gownaris *et al*, 2018). No reliable recent figures are available for both catch and effort in Turkana fisheries to estimate the effects of recent variations on fish stocks. Data from the 1980's show a strong linear relationship between deviations of lake levels from long-term mean and annual catch per boat in tons (Kolding 1992). Following this relationship, fish catch would decrease 4 tons per boat per year per meter lake level decrease (J. Kolding pers. comm.). The average boat catches about 20 tons of fish per year (Kolding, 1992). The decrease in average seasonal variation by about 50 cm, observed since 2015 would mean 10% loss of income and/ or food for people depending on fisheries around Lake Turkana. For people who live in poverty, these 10% can be existential, unless other sources of income and nutrition become available.

## River channels through the Omo delta as indicators for ecosystem service delivery

The contemporary Omo delta is a very young formation, built up through an interplay between sediment deposition from the Omo river and wave energy in Lake Turkana (Butzer 1970). Due to the availability of fertile land and fresh water from the river, the delta area is densely populated by communities of the Dassanech tribe, who graze their animals and conduct flood recession agriculture there. Throughout the 1970's and 80's the river channel through the newly deposited delta has followed strong dynamics, but since the 90's a consolidation of the channel has started, with sedimentation taking place primarily at the river mouths (Figure 15). Dam-like deposits along the river channel keep the river in a stable bed and are due to their flood-safe elevation the most important sites where people settle. We used the length of the river channels as an indicator for the overall amount of ecosystem services provided in the delta area. The overall length of the channels strongly correlates with the extent of the delta. In line with the observations of continuously high lake extents in the northern part of lake Turkana, the decreasing overall channel length since 2012 indicates that the delta is shrinking. Upstream sediment trapping behind the new dams Gibe III (closed in 2015) but also the Kuraz irrigation system (start of operation in 2012) may be the most important reason for reduced sediment loads. This does not mean that people who currently live there are already threatened by the shrinking delta, but it may provide an indication that the growing function of the delta as a refuge for people who lost their livelihoods elsewhere is coming to a halt. This is worrying given the future prospects of simultaneously decreasing fish stocks, area of flood recession agriculture and availability of non-saline grazing land.



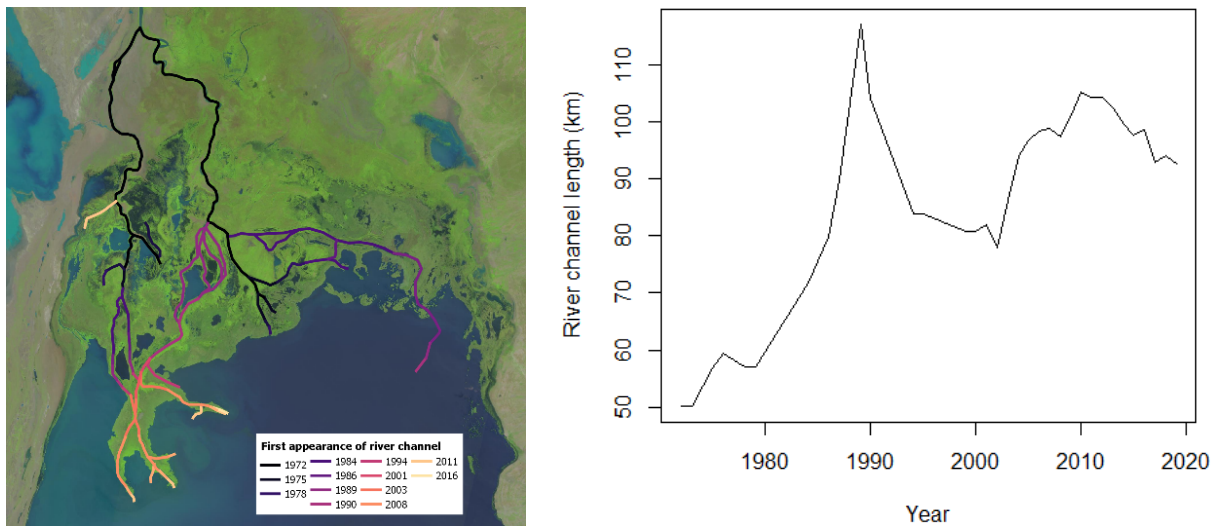


Figure 15 – Length of the river channels within the Omo delta from 1972 to 2019. Left: Year of first appearance, right: total length.

### Implications of reduced flow dynamics and sedimentation<sup>4</sup> for delta vegetation

As shown above, the equalized flows of the Omo river have led to a reduction in seasonally flooded area. This effect was most pronounced in the Omo Delta, where the flooded area decreased from a peak of >80 km<sup>2</sup> in 2014 to a stable low of <20 km<sup>2</sup> in 2016, 2017 and 2018 (Figure 16 C). Low rainfalls in 2015 and 2016 exacerbated this effect.

The Leaf Area Index (LAI) in the seasonally flooded parts of the delta has increased more or less continuously since 2013, and so has the variability within each year (Figure 16). This indicates that the lake water was “eating” into the already vegetated parts of the delta, supported by the strong winds that typically blow from a southerly direction in this region (Schuster and Nutz, 2018). The reduction in seasonal floods arriving through the Omo river and the encroachment of salty lake water have put pressure on the delta from two sides, with strong implications for the people who live in and out of the delta, where they graze their livestock and grow their food.

To find out more about the temporal dynamics of the delta vegetation, we conducted an unsupervised vegetation classification based on k-means using the RStoolbox package in R. Over a monthly LAI time series from Sentinel 2 imagery, we identified six clearly distinguishable classes (Figure 17) that again belong to three general groups. Classes 1 and 3 form the youngest part of the delta, on the recently deposited soils at the end of the Omo river. They show the greatest seasonal variations in LAI, resulting from regular flooding. Yet, the vegetation signal slopes upwards, indicating that more water is evaporating than newly coming in. Since the flooding patterns are changed by the Gibe III dam, vegetation is currently able to grow on previously flooded areas. Class 1 is strongly affected by the explosive growth of the invasive shrub *Prosopis juliflora* that forms dense and thorny thickets and has high salt tolerance levels. Classes 2 and 4 are closest to the lake and are dominated by halophytic (salt-tolerant) vegetation. They remained stable during the observation period, but are of low importance for human uses. Classes 5 and 6 are located in the Northern part of the delta, furthest away from the lake, comprised of forest (Class 5) and shrubland (Class 6). They show a decreasing LAI trend over time. It is unclear, what leads to this reduction, but in general this area is rarely flooded and vegetation may depend mostly on groundwater reserves. Classes 1, 3 and 5 are most important for ecosystem services, as the majority of people in the delta lives along the two main streams of the river located here, where freshwater is available. In the absence of fresh water inputs from floods due to hydrological alterations of the natural flow regime, previously used areas will increasingly dry out or get under the influence of salty lake

<sup>4</sup> For more on the sediment modelling, see the appendix



water. This will impede crop growth and facilitate invasions of previously grazed grasslands with shrubs, which has strong implications for the livelihoods of people.

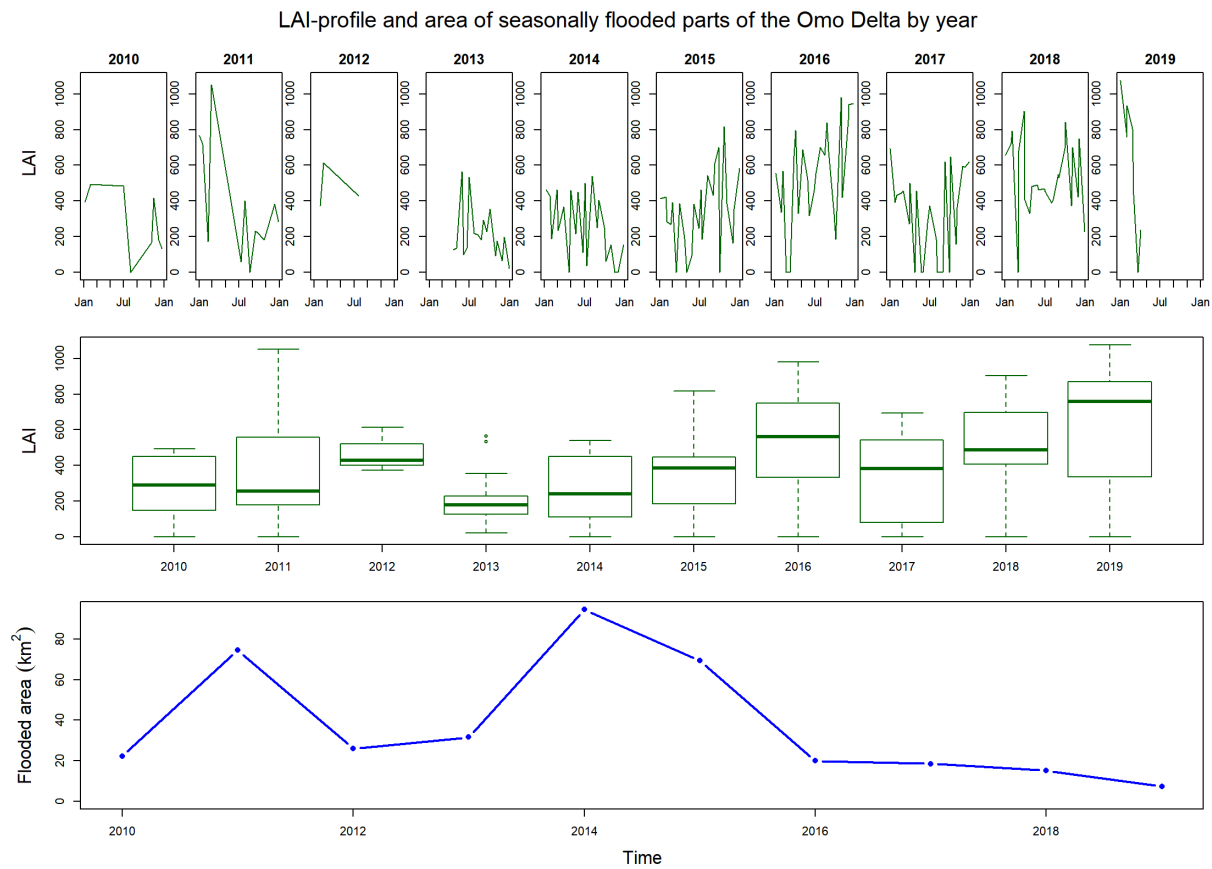


Figure 16 – Leaf Area Index (LAI) inside annually flooded areas of the Omo Delta and their size.

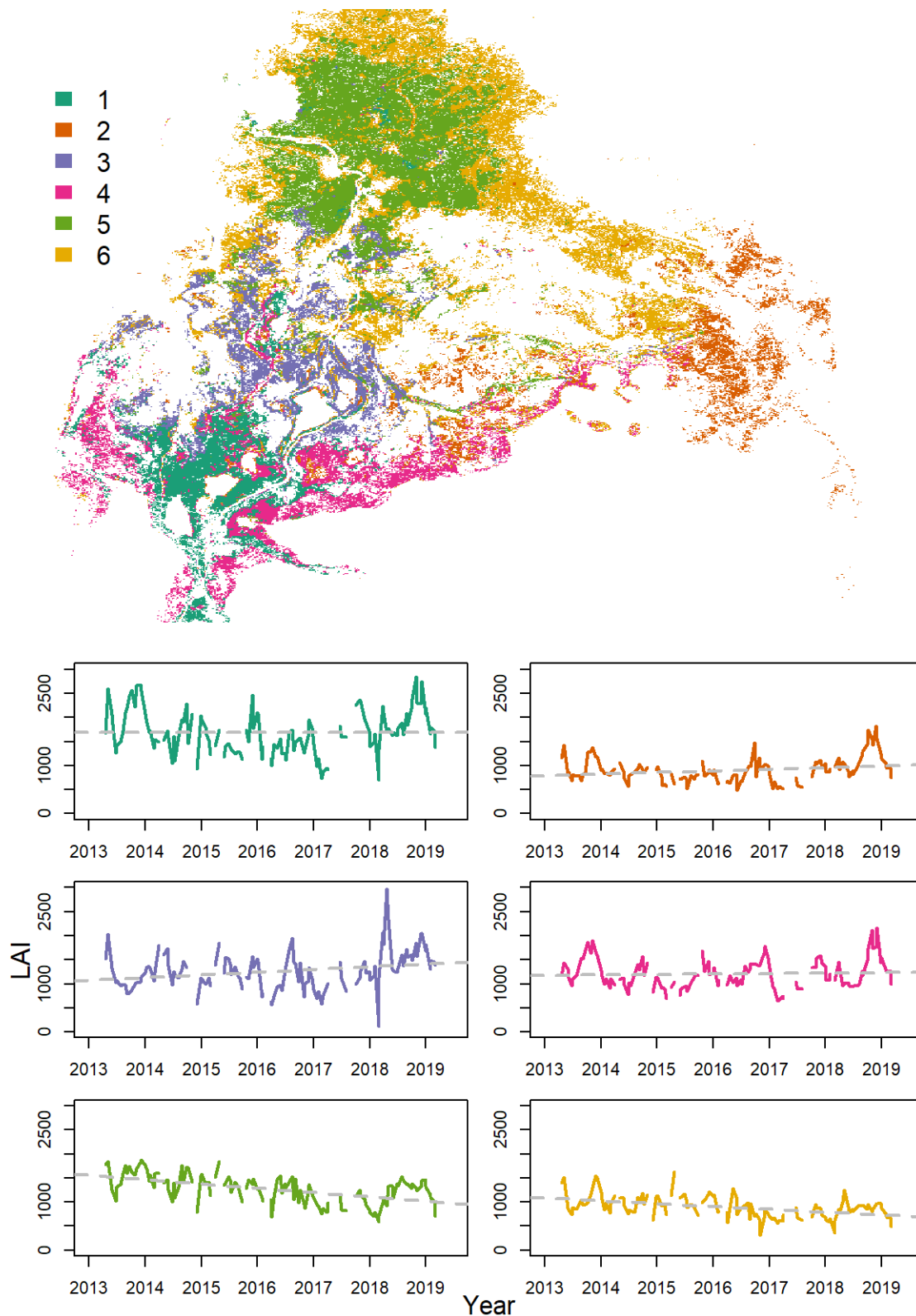


Figure 17 – Unsupervised vegetation classification for the Omo delta based on LAI time series derived from Landsat and Sentinel 2 imagery. Shown are six classes with their respective LAI time series. Linear regression lines are added to aid visual interpretation. White areas of the map are not classified due to generally low vegetation signal from inundation or they are part of the desert.

## Omo riparian forests

Despite the arid climate, the riparian areas of the lower Omo river support dense forest of up to 20 m height (Carr, 1998). These forests are important for ecosystem services as they give shelter, support year-round grazing, charcoal/ wood for cooking and other non-timber forest products. These forests can only exist due to the water table provided by the river. This is shown by mean LAI values that follow the same seasonal variation depending on rainfall but decrease gradually with distance to the Omo River (Figure 18).

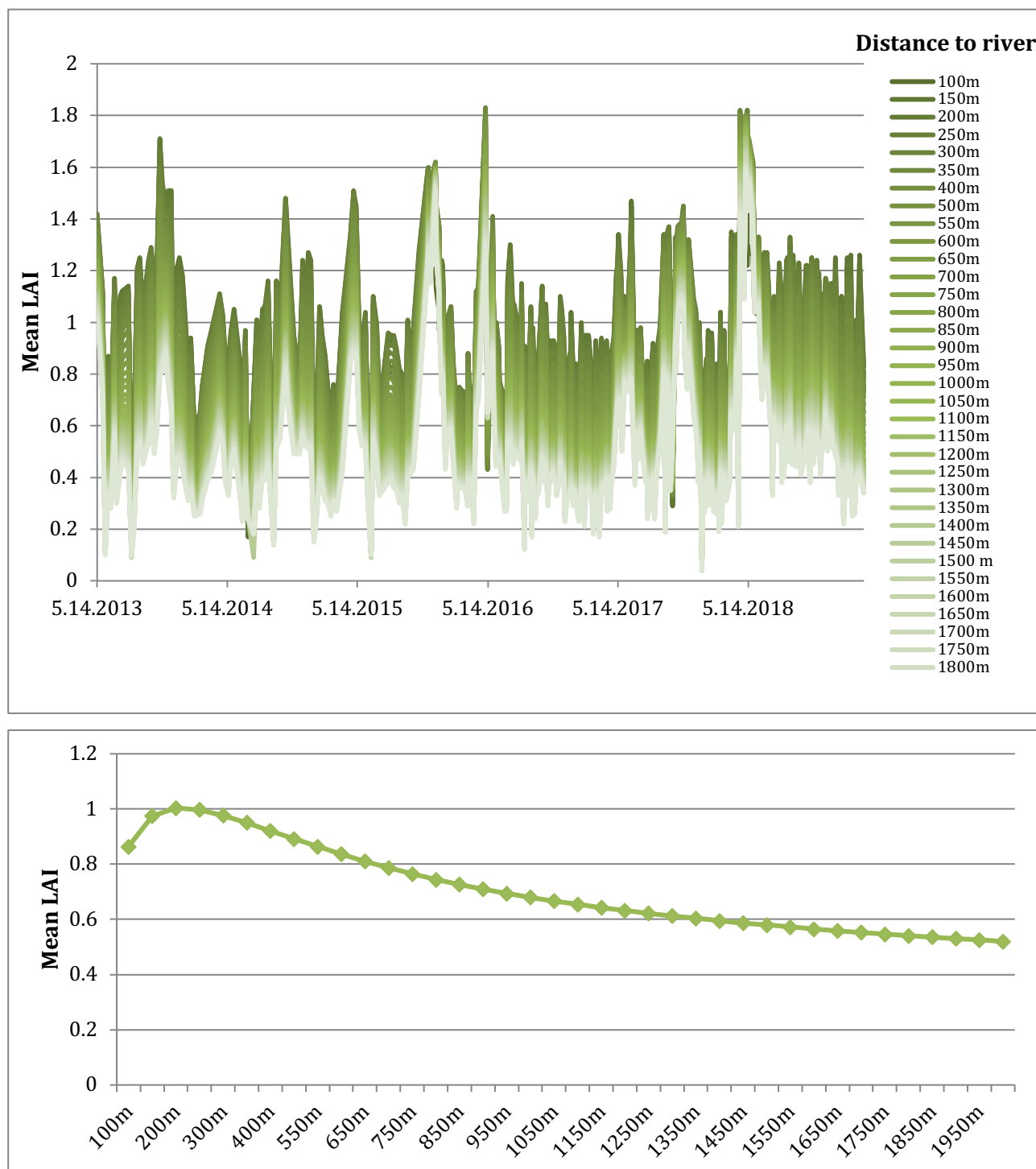


Figure 18 – Leaf area index variation within buffers in 100 m increments around the lower Omo River based on Sentinel 2 imagery. Top: development over time, bottom: average across years. Data by VISTA remote sensing.

We compared remotely sensed LAI values between the dry and the wet season by year (Figure 19). Areas with higher values in the dry season are those supported by river water, either through flooding and irrigation or through the groundwater. This shows the dependence of the riparian forests on the river water in addition to the seasonal rainfall. We will use *groundwater storage volumes* simulated by the TOPKAPI-ETH model to determine future changes in riparian forests under changes flow conditions. Overall lower flow rates could lead to a reduction in groundwater levels with implications for the extent and the quality of the riparian forests.

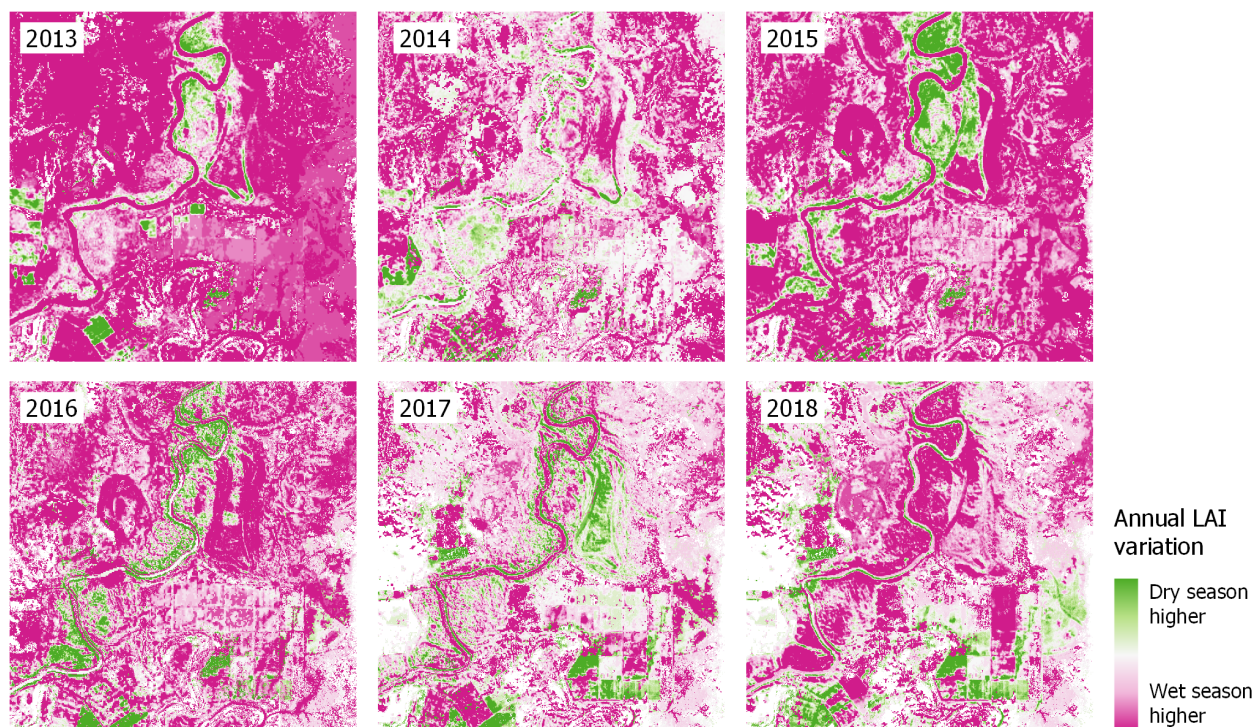


Figure 19 – Difference in Leaf Area Index (LAI) between Landsat 8 and Sentinel 2 images taken in the dry and the wet season. Pink areas show higher values in the wet season, green areas higher values in the dry season due to irrigation (lower part of the image) and ground water provided by the river.

### Flood recession agriculture

Flood recession agriculture is of high importance for the food security of pastoralist communities in the lower Omo valley (Yazew *et al* 2015, Yntiso 2012). Based on high resolution RapidEye satellite imagery, we digitized the cultivated area in temporarily flooded zones along the river for the years 2005, 2008, 2010, 2011 and 2012. We found a strong correlation between the modelled annual discharge variation and flood recession area (Figure 20). The  $\delta$  is the average, for all TOPKAPI-ETH cells in the analysis, of the difference of the two "Q"s (which indicate the seasonal flood and the secondary "damaging" one). This relationship allows us to predict changes in flood recession area under different modelled flow scenarios.

A more long-term account of the state of recession agriculture in the Dassanech woreda (which includes the lowest part of the Omo and the delta) shows strong fluctuations in cultivated area from year to year with by far the lowest values reported in 2017 and 2018 (Table 9). The results of a 2019 field-based account confirm this trend as shown in Figure 21.

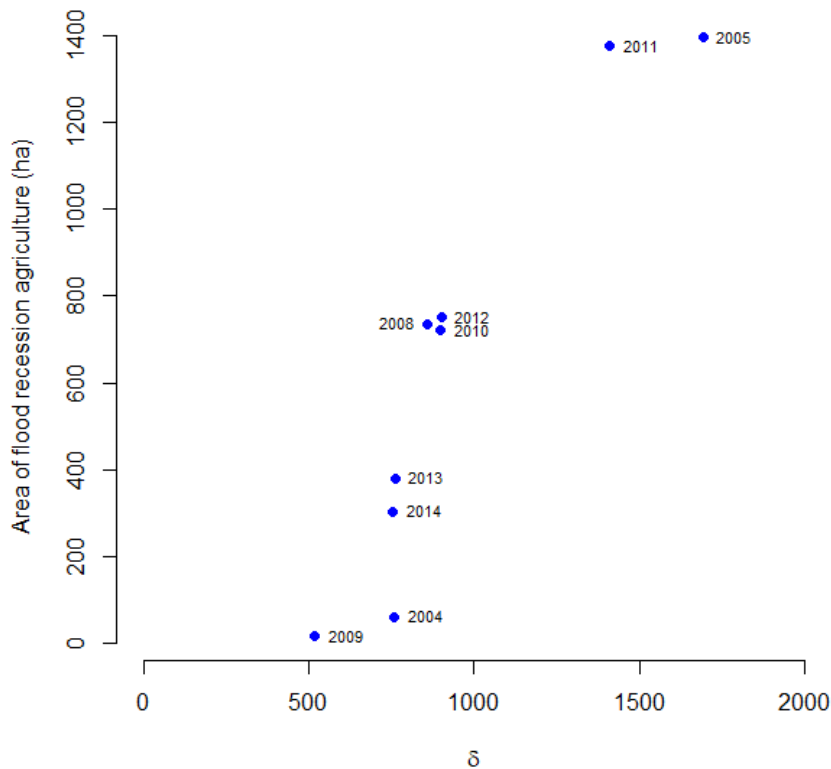


Figure 20 – Relationship between observed flood recession agriculture area and modelled discharge in the lower Omo (data provided by F. Semeria, POLIMI).

Table 9 – Area (ha) of flood recession agriculture in the Dassanech woreda reported by different sources

Year	RS observations (F. Semeria)	Yntiso (2012)	Data from woreda administration (un- published)	Field observations (F. Kleinschroth)
2006	1712.8			
2007		650.7		
2008	736.1			
2009		501.0		
2010	721.2	397.3		
2011	1376.1	1052.2	1045.6	
2012	751.5		821.5	
2013	379.3		340.2	
2014	303.7			
2015				
2016				
2017			191.6	
2018			30.2	
2019				203



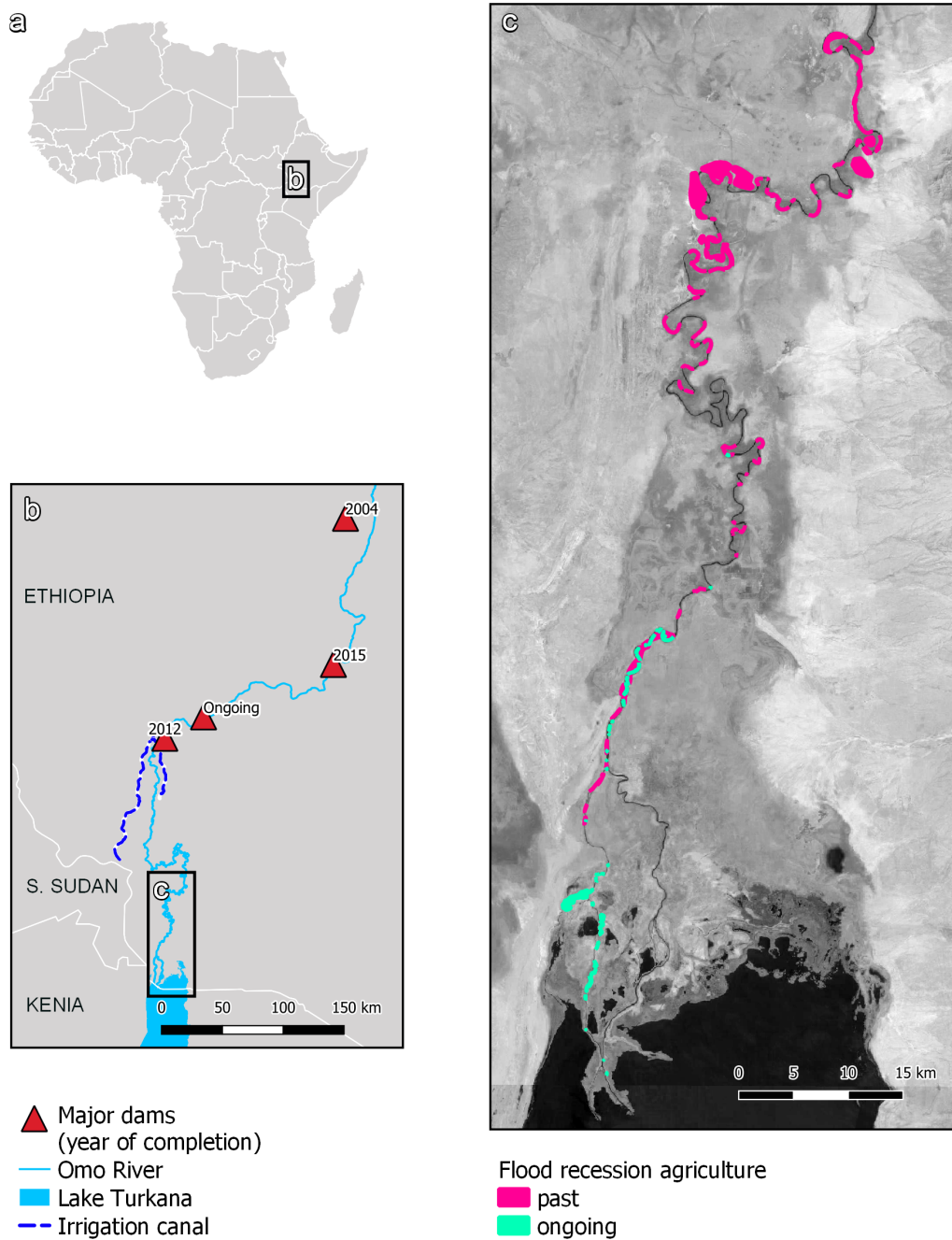


Figure 21 – Field-based account of ongoing flood-recession agriculture (March 2019, only the western branch of the river in the delta was covered) compared to abandoned areas that were detected with active cultivation on high resolution imagery from 2011.

## Summary

Our observations from the Omo-Turkana basin highlight far-reaching changes in ecosystem service potential for people who directly depend on fisheries, flood recession agriculture and grazing. The combined effect of lacking decadal floods, reduced seasonal water level variation, loss of land area and salt water encroachment in the delta pose an imminent threat to livelihoods.

Further testing of vegetation responses to different scenarios of climate change, reservoir operation policies, hydrologic regimes and agriculture intensities is still missing, as the hydrologic modeling is still ongoing. While long-term climatic variations may be more pronounced than dam-induced changes, the impact on seasonal effects in river flow and lake levels can already be observed.

Based on the evidence of our findings and on the complete lack of ground data to establish cause-effect relationships and/or models between changes in river flows and lake levels and ecosystem and their services, we will rely on models of impacts on ecosystems based on the post-processing of the output of the extended hydrological model (e.g. including the GLM module). This is for instance the case of the “Index of Hydrologic Alteration, IHA” (e.g. Richter *et al.*, 1996; 1997), which can quantify impacts on river components such as those already observed.

The WEF simulations including the quantification of indexes that are proxy for impacts on ecosystems will direct by the end of the project to discuss mitigation actions, which likely should include ongoing work on timing and control of filling of the planned Koysha dam as well as on potential environmental flow releases, both crucial to avoid impacts additional to those observed so far. The DAF-computed reservoir operating policies may also identify further actions on the existing systems that will help restoring some localized flood events in the delta. Moreover, additional measures such as artificial deviations of the riverbed of the Omo could be considered, to ensure some flooding in the delta area and allow local populations to continue using these areas before soil salinity becomes too high.

#### 4. SUBSET OF INDICATORS COMPUTABLE WITH WEF MODEL COMPONENTS

Following the formulation of the WEF model, we present in this section the indicator tables with indicators that we cannot compute from the WEF filtered out.

##### 4.1 OMO-TURKANA BASINS

Tables 10 through 13 present the evaluation indicators to be computed for the OTB for each of the four major water use sectors (Energy, Food, Water and Ecosystem services, and Socio-economic).

Table 10 – OTB Energy indicators to be computed by the WEF model

ID	Short description	Definition
i_E_1	Energy production from hydro-power	Annual mean energy production in the Omo basin over the time horizon
i_E_2	Energy production from each power plant	Annual mean energy production for each power plant over the time horizon
i_E_3	Deficit with respect to energy demand	Annual mean energy deficit for each country in the Omo-Turkana basin over the time horizon

Table 11 – OTB Food indicators to be computed by the WEF model

ID	Short description	Definition
i_F_2	Yield of rain fed crops in terms of tons/ ha	Amount of crop produced per ha under current and future conditions
i_F_3	Yield of irrigated crops in terms of tons/ha	Amount of crop produced per ha under current and future conditions
i_F_4	Yield of rain fed and irrigated crops in terms of proteins/ ha	Amount of proteins produced per ha under current and future conditions
i_F_5	Yield of rain fed and irrigated crops in terms of calories/ ha	Amount of calories produced per ha or site or basin under current and future conditions

(Table 11 continued)

i_F_6	Water productivity of rain fed crops	Amount of water used to produce a unit of crop
i_F_7	Water productivity of irrigated crops	Amount of water used to produce a unit of crop
i_F_8	Irrigation water required for optimal production of irrigated crops	
i_F_16	Dietary supply adequacy - calories from crops, livestock and fisheries	Key indicator to estimate if food targets are being met . Formula: (calories produced in spatial unit/ population count) * calorie demand per capita
i_F_17	Dietary supply adequacy - proteins from crop, livestock and fisheries	Key indicator to estimate if food targets are being met . Formula: (proteins produced in spatial unit/ population count) * protein demand per capita

Table 12 – OTB Water and Ecosystem indicators to be computed by the WEF model

ID	Short description	Definition
i_W_Ec_1	Magnitude of flooding	Surface water dynamics
i_W_Ec_2	Duration of flooding	
i_W_Ec_3	Water requirements for Habitat and fish migration	Seasonal flow patterns needed to maintain habitats and connectivity for fish species
i_W_Ec_4	Sediment transport	Amount of sediment eroded, transported by rivers, trapped behind dams, deposited in floodplains
i_W_Ec_5	Lake levels: Indicator for long-term variability of climate and water use patterns	Average lake levels should not be permanently below 362.3 masl, otherwise Ferguson's gulf will permanently dry out, with negative effects on fish stocks (Gownaris 2017)
i_W_Ec_7	River discharge: Amount of flow at different river cross-sections in the basin	Baseline discharge statistics at Gibe III location shown in the diagram below. Average discharge values 1964-2001 (Jan: 78; Feb: 71; Mar: 61; Apr: 86; May: 141; Jun: 336; Jul: 942; Aug: 1529; Sep: 1058; Oct: 584; Nov: 217; Dec: 117)
i_W_Ec_8	Index of Hydrological alteration	Alteration of the hydrological regime with respect to a given reference
i_W_Ec_9	Evaporation rate from water bodies	
i_W_Ec_10	Water table (surface and groundwater level)	

Table 13 – OTB Socio-economic indicators to be computed by the WEF model

ID	Short description	Definition
i_SE_1	Population	total number of people
i_SE_2	Population Density	people per sq. km of land area
i_SE_3	Population by gender	total number of males, total number of females
i_SE_4	Population by age	total number of people aged 0-14, total number of people aged 15-64, total number of people aged 65 and over
i_SE_5	Population growth rate	% annual rate of change in population
i_SE_6	Population growth rate - urban	% annual rate of change in population in urban areas
i_SE_7	population growth rate - rural	% annual rate of change in population in rural areas



## 4.2 ZAMBEZI RIVER BASIN

Tables 14 through 17 present the evaluation indicators to be computed for the ZRB for each of the four major water use sectors (Energy, Food, Water and Ecosystem services, and Socio-economic).

Table 14 – ZRB Energy indicators to be computed by the WEF model

ID	Short description	Definition
i_E_1	Energy production from hydro-power in river basin	The indicator measures yearly average performance in term of energy production from all the plants in the River Basin.
i_E_2	Energy production from hydro-power at national level	The indicator measures yearly average performance in term of energy production from all the plants of a given country.
i_E_3	Energy production from each hydro-power plant	The indicator measures yearly average performance in term of energy production of a given power plant
i_E_4	Deficit with respect to energy demand in the river basin	The indicator measures yearly average deficit with respect to the energy demand related to all the plants in the River Basin.
i_E_5	Deficit with respect to energy demand at national level	The indicator measures yearly average deficit with respect to the energy demand related to all the plants in a given country.
i_E_6	Deficit with respect to energy demand for each power plant	The indicator measures yearly average deficit with respect to the energy demand related to a given power plant

Table 15 – ZRB Food indicators to be computed by the WEF model

ID	Short description	Definition
i_F_2	Yield of rain fed crops in terms of tons/ ha	Amount of crop produced per ha under current and future conditions
i_F_3	Yield of irrigated crops in terms of tons/ha	Amount of crop produced per ha under current and future conditions
i_F_4	Yield of rain fed and irrigated crops in terms of proteins/ ha	Amount of proteins produced per ha under current and future conditions
i_F_5	Yield of rain fed and irrigated crops in terms of calories/ ha	Amount of calories produced per ha or site or basin under current and future conditions
i_F_6	Water productivity of rain fed crops	Amount of water used to produce a unit of crop
i_F_7	Water productivity of irrigated crops	Amount of water used to produce a unit of crop
i_F_8	Irrigation water required for optimal production of irrigated crops	
i_F_13	Total fish catch and production	tons of fish produced or caught on a per hectare basis
i_F_14	Calorie yield from fish catch and production	Output in terms of calories, all species combined, losses considered as in (biomass(kg) * calories/kg) -losses (kg) per hectare
i_F_15	Protein yield from fish catch and production	Output in terms of proteins, all species combined, losses considered as in (biomass(kg) * calories/kg) -losses (kg) per hectare

(Table 15 continued)

i_F_16	Dietary supply adequacy - calories from crops, livestock and fisheries	Key indicator to estimate if food targets are being met . Formula: (calories produced in spatial unit/ population count) * calorie demand per capita
i_F_17	Dietary supply adequacy - proteins from crop, livestock and fisheries	Key indicator to estimate if food targets are being met . Formula: (proteins produced in spatial unit/ population count) * protein demand per capita

Table 16 – ZRB Water and Ecosystem indicators to be computed by the WEF model

ID	Short description	Definition
i_W_Ec_1	Magnitude of flooding	Surface water dynamics
i_W_Ec_2	Duration of flooding	
i_W_Ec_3	Water requirements for Habitat and fish migration	Seasonal flow patterns needed to maintain habitats and connectivity for fish species
i_W_Ec_4	Sediment transport	Amount of sediment eroded, transported by rivers, trapped behind dams, deposited in floodplains
i_W_Ec_6	River discharge: Amount of flow at different river cross-sections in the basin	
i_W_Ec_7	Index of Hydrological alteration	Alteration of the hydrological regime with respect to a given reference
i_W_Ec_8	Evaporation rate from water bodies	
i_W_Ec_9	Water table (surface and groundwater level)	
i_W_Ec_10	water temperature alterations	difference of temperature between the upstream and downstream water temperature in °C.
i_W_Ec_11	dissolved oxygen	difference of temperature between the upstream and downstream water temperature in °C.

Table 17 – ZRB Socio-economic indicators to be computed by the WEF model

ID	Short description	Definition
i_SE_1	Population	total number of people
i_SE_2	Population Density	people per sq. km of land area
i_SE_3	Population by gender	total number of males, total number of females
i_SE_4	Population by age	total number of people aged 0-14, total number of people aged 15-64, total number of people aged 65 and over
i_SE_5	Population growth rate	% annual rate of change in population
i_SE_6	Population growth rate - urban	% annual rate of change in population in urban areas
i_SE_7	population growth rate - rural	% annual rate of change in population in rural areas

## 5. CONCLUSIONS

The main objective of this report was to provide a description of the integrated Water, Energy and Food (WEF) model in the context of the DAFNE framework for analysing and evaluating the nexus. We provided an overview of the interconnections between the DAFNE stakeholder participatory process and the resulting WEF nexus indicators, and the modelling framework.

As mentioned in the report, the purpose of the WEF model, is to evaluate in detail the full set of indicators in a spatially distributed manner. To do this, the WEF has at its core a spatially distributed hydrological model that accounts for both the hydrological fluxes and anthropogenic activities in the basin. The hydrological model is linked with various complimentary models to allow the computation of evaluation indicators that are not directly obtained from the outputs of the hydrological model. The latter are further postprocessed to compute derived indicators, for those compartments of the nexus, for which models do not yet exist and the development of which clearly exceeds the scope of the DAFNE project.

In the coming months we will refine the details, and produce a full final suite of indicators for the case study basins to aid decision makers in choosing between different future development trajectories.

## 6. REFERENCES

- Allen R., Pereira L., Raes D. and M. Smith, (1998), Crop evapotranspiration – Guidelines for computing crop water requirements, *FAO Irrigation and drainage paper* 56
- Avery S T and Tebbs E J 2018 Lake Turkana, major Omo River developments, associated hydrological cycle change and consequent lake physical and ecological change J. Great Lakes Res. 44 1164–82 Online: <https://doi.org/10.1016/j.jglr.2018.08.014>
- Butzer K W 1970 Contemporary Depositional Environments of the Omo Delta Nature 226 425–30
- Calamita E., Vanzo D., Wehrli B. and M. Schmid, (2019) Can management opportunities reduce impacts of large tropical dams on downstream water quality?, Manuscript in preparation
- Carr C J 1998 Patterns of vegetation along the Omo River in Southwest Ethiopia Plant Ecol. 135 135–63
- Gownaris N J, Pikitch E K, Aller J Y, Kaufman L S, Kolding J, Lwiza K M M, Obiero K O, Ojwang W O, Malala J O and Rountos K J 2017 Fisheries and water level fluctuations in the world's largest desert lake Ecohydrology 10 1–16
- Gownaris N J, Rountos K J, Kaufman L, Kolding J, Lwiza K M M and Pikitch E K 2018 Water level fluctuations and the ecosystem functioning of lakes J. Great Lakes Res. 44 1154–63 Online: <https://doi.org/10.1016/j.jglr.2018.08.005>
- Hodobod J, Stevenson E G J, Akall G, Akuja T, Angelei I, Bedasso E A, Buffavand L, Derbyshire S, Eulenberger I, Gownaris N, Kamski B, Kurewa A, Lokuruka M, Mulugeta M F, Okenwa D, Rodgers C and Tebbs E 2019 Social-ecological change in the Omo-Turkana basin: A synthesis of current developments Ambio Online: <http://link.springer.com/10.1007/s13280-018-1139-3>
- Junk W, Bayley P B and Sparks R E 1989 The flood pulse concept in river-floodplain-systems Can. J. Fish. Aquat. Sci. 106 110–27
- Kolding J 1992 A summary of Lake Turkana: an ever-changing mixed environment Mitt. Internat. Verein. Limnol. 23 25–35
- Kolding J and van Zwieten P A M 2012 Relative lake level fluctuations and their influence on productivity and resilience in tropical lakes and reservoirs Fish. Res. 115–116 99–109 Online: <http://dx.doi.org/10.1016/j.fishres.2011.11.008>
- Richter, B.D., Baumgartner, J.V., Powell, J., and Braun, D.P., (1996). A method for assessing hydrologic alteration within ecosystems. Conservation Biology, 10(4), 1163-1174.
- Richter, B.D., Baumgartner, J.V., Wigington, R., and Braun, D.P. (1997). How much water does a river need? Freshwater Biology, 37, 231-249.
- Schuster M and Nutz A 2018 Lacustrine wave-dominated clastic shorelines: modern to ancient littoral landforms and deposits from the Lake Turkana Basin (East African Rift System, Kenya) J. Paleolimnol. 59 221–43
- Schwatke C, Dettmering D, Bosch W and Seitz F 2015 DAHITI - An innovative approach for estimating water level time series over inland waters using multi-mission satellite altimetry Hydrol. Earth Syst. Sci. 19 4345–64
- Vanuytrecht E., Raes D., Steduto P., Hsiao T.C., Fereres E., Heng L.K., Vila M.G. and P.M. Moreno, (2014), AquaCrop: FAO's crop water productivity and yield response model, *Environmental Modelling & Software*

- Yazew E, Mezgebu A, Embaye T G, Teka D and March E 2015 Multi Reservoir Operation and Challenges of the Omo River Basin : Part II : Potential Assessment of Flood Based Farming on lower Omo Ghibe Basin (Mekelle, Ethiopia: Spate Irrigation Network Foundation)
- Yntiso G 2012 Environmental Change , Food Crises and Violence in Dassanech , Southern Ethiopia (Berlin: Freie Universität Berlin, Research Unit Peace and Conflict Studies)

## APPENDIX – OTB SEDIMENT MODELLING RESULTS

The TOPKAPI-ETH hydrological model has been complemented with a soil erosion and sediment transport module, to simulate sediment dynamics at the catchment scale. This fully-distributed physically-based numerical model constitutes a novel approach to study the sediment balance over large basins, because it allows to account for the spatial gradients of erosion drivers, such as meteorological forcing, and surface characteristics, such as land cover and soil erodibility. In very large basins, such as the case studies of the ZRB and ORB, these gradients are of primary importance to define the role of the different basin regions in producing, transporting or depositing sediments.

Here we present an application of the hydrological model and the new sediment module to the ORB. Since no precise information has been found so far that clarifies if the reservoirs present in the basin (i.e. Gibe I and Gibe III) have a strategy to release the incoming sediments, at this stage we performed two simulations to account for the two extreme cases: The Scenario A assumes that dams don't retain any of the inflowing sediment, while in the Scenario B the dams retain 100% of the incoming sediment. The dams which have been taken into account are Gibe I and Gibe III.

As presented in detail in D3.1, soil erosion in the model can be simulated with a transport capacity approach, or assuming that the sediment discharge can be different than the transport capacity and proportional to the bed shear stress of the overland flow or its stream power. In this application we chose the transport capacity approach, thus assuming that the sediment discharge always equal transport capacity of the overland flow, computed following Prosser and Rustomij (2000):

$$T_{C-E} = \alpha S^{\beta} q^{\gamma}. \quad (1)$$

The  $\beta$  and  $\gamma$  parameters have been assumed equal to 1.4, as suggested by Prosser and Rustomij (2000). The  $\alpha$  parameter, which summarizes the land surface and soil characteristics, has been assumed spatially distributed, to account for the heterogeneity of land cover and soil type across the basin. The spatial distribution of  $\alpha$  has been derived from the intersection of the maps of the land cover and management factor of the Universal Soil Loss Equation (C factor) and the soil erodibility factor of the same equation (K factor). These maps are available from the work of Borrelli et al. (2013) and are shown in figure X for the ORB.

The final  $\alpha$  value is computed as

$$\alpha = \alpha_1 C K, \quad (2)$$

where  $\alpha_1$  is the actual calibration parameter, defining the magnitude of sediment production on the hillslopes.

Fine sediment advection in the channel is modelled as

$$\frac{\partial AC}{\partial t} + \frac{\partial QC}{\partial x} - S_{bed} = 0 \quad (3)$$

Where  $A$  is the area of the river cross section,  $C$  the fine sediment concentration average on the cross section,  $Q$  the river discharge and  $S_{bed}$  the term of sediment exchange with the bed. In our simulations the term  $S_{bed}$  has been assumed equal to zero, meaning that no deposition is allowed on the river bed. We acknowledge that this assumption neglects an important process of the sediment dynamics in our system, however the lack of any measurement on the main channel of the Omo river, and especially close to the outlet in Lake Turkana, does not allow calibration of this term.

For calibration, estimates of annual sediment load at 6 stations (see Figure A.1) in the Gilgel Gibe River subbasin of the OTB were available from grab sample measurements carried out in 2010 and 2011 (reported in Vanmaercke et al., 2014). 4 of these stations are located on the main tributaries of Gibe I reservoir (stations G\_I 1 to G\_I 4 in Figure A.1), therefore we used these data to estimate a total sediment load into the reservoir and calibrated the model on the period 2010-2011 in order to match this load. In Table A.1 the measured and modelled sediment load into Gibe I is reported, together with the loads at the single stations.

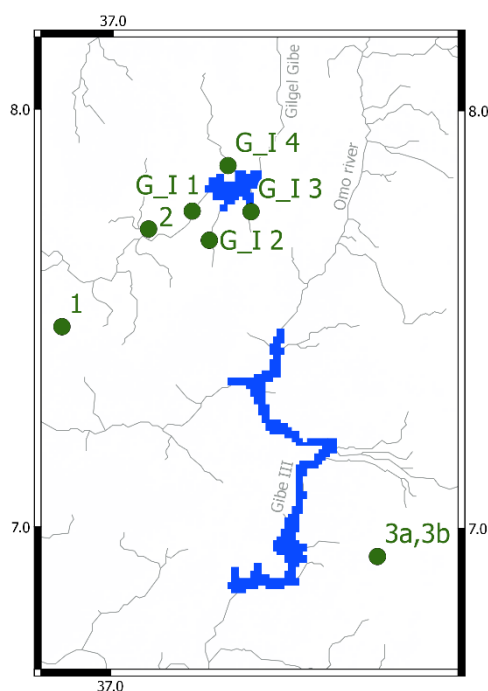


Figure A.1 – Location of the stations where annual sediment loads and of the lake formed by the Gibe III dam

It is important to notice that the calibration has been carried out on the aggregated value of the stations G\_I 1 to G\_I 4 and not at the level of the single station, therefore high errors at the single stations are to be expected. In our approach, the relative contribution of the single cells, and therefore of the subbasin, is fixed by the *C* and *K* factors of the USLE equation and has not been subject to calibration as this would introduce a disproportionate number of degrees of freedom against the very sparse measurements available in the study area.

Table A.1 – Measured vs modelled sediment load

	Mean annual sediment load [t/y]		Error [%]
	<i>Measured</i>	<i>Modelled</i>	
<b>Sediment load into Gibe I</b>	$123.31 \cdot 10^4$	$1.2151 \cdot 10^4$	-2
<b>Station G_I 2</b>	$9.30 \cdot 10^4$	$2.79 \cdot 10^4$	-70
<b>Station G_I 1</b>	$76.39 \cdot 10^4$	$95.12 \cdot 10^4$	25
<b>Station G_I 3</b>	$17.41 \cdot 10^4$	$16.11 \cdot 10^4$	-7
<b>Station G_I 4</b>	$20.21 \cdot 10^4$	$7.49 \cdot 10^4$	-63
<b>Station 1</b>	$70.79 \cdot 10^4$	$14.29 \cdot 10^4$	-80
<b>Station 2</b>	$34.25 \cdot 10^4$	$18.90 \cdot 10^4$	-45
<b>Station 3a</b>	7.96	0	100
<b>Station 3b</b>	86.76	0	100

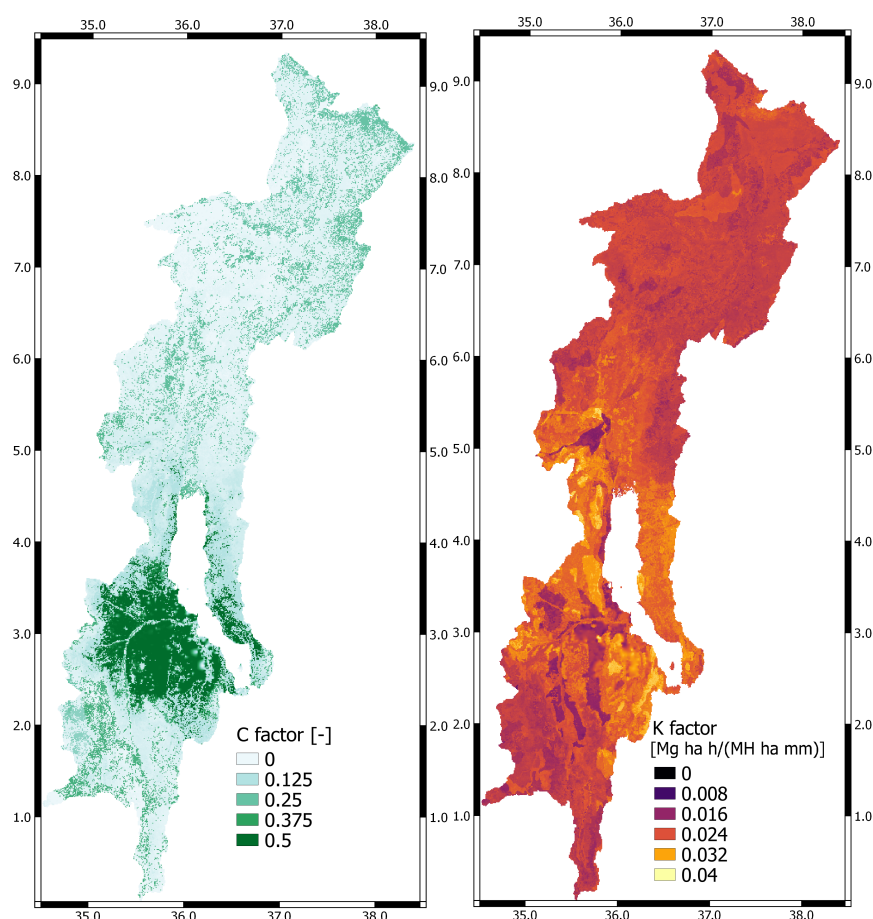


Figure A.2 – Spatial distribution of the C and K USLE factors

The model was then run on the period 1-Jan-2015 – 30-Oct-2018 in the two scenarios of sediment trapping. The year 2015 is considered a warm-up period for the model and thus results are analysed for the years 2016 to 2018.

The total soil erosion and deposition produced by the four years of simulation is reported in Figure A.2. The spatial distribution shows that most of the erosion of the hillslopes takes place in the northern region of the basin and in the southernmost point. Deposition on the hillslopes is also mostly observed in these areas, as we expect due to the transport capacity assumption of our model, which implies that higher sediment mobilization also induces stronger deposition in locations of slope or land use change.

In Figure A.2, the frequency distribution of erosion and deposition values of the single cells are also reported for three latitudinal regions of the basin comprised between 0 and 3.3°N, 3.3 and 6.6°N and 6.6 and 9.9°N. The histograms show that in the central region the frequency of very small erosion and deposition values close to zero is higher than in the northern and southern regions. In particular, the northern region shows the highest frequency for high erosion values.

This map is the same for the 0% sediment trapping and the 100% sediment trapping scenario, as the processes on the hillslopes are independent of the dams functioning.

We observe that, as higher sediment production is observed in the upstream areas of the main rivers of the OTB, stronger deposition in the main channel is expected in the central region of the basin, compared to the northern and southern one. As mentioned in the main report, this process is not simulated by the model, however it is believed to have an important role in the sediment balance of the basin.



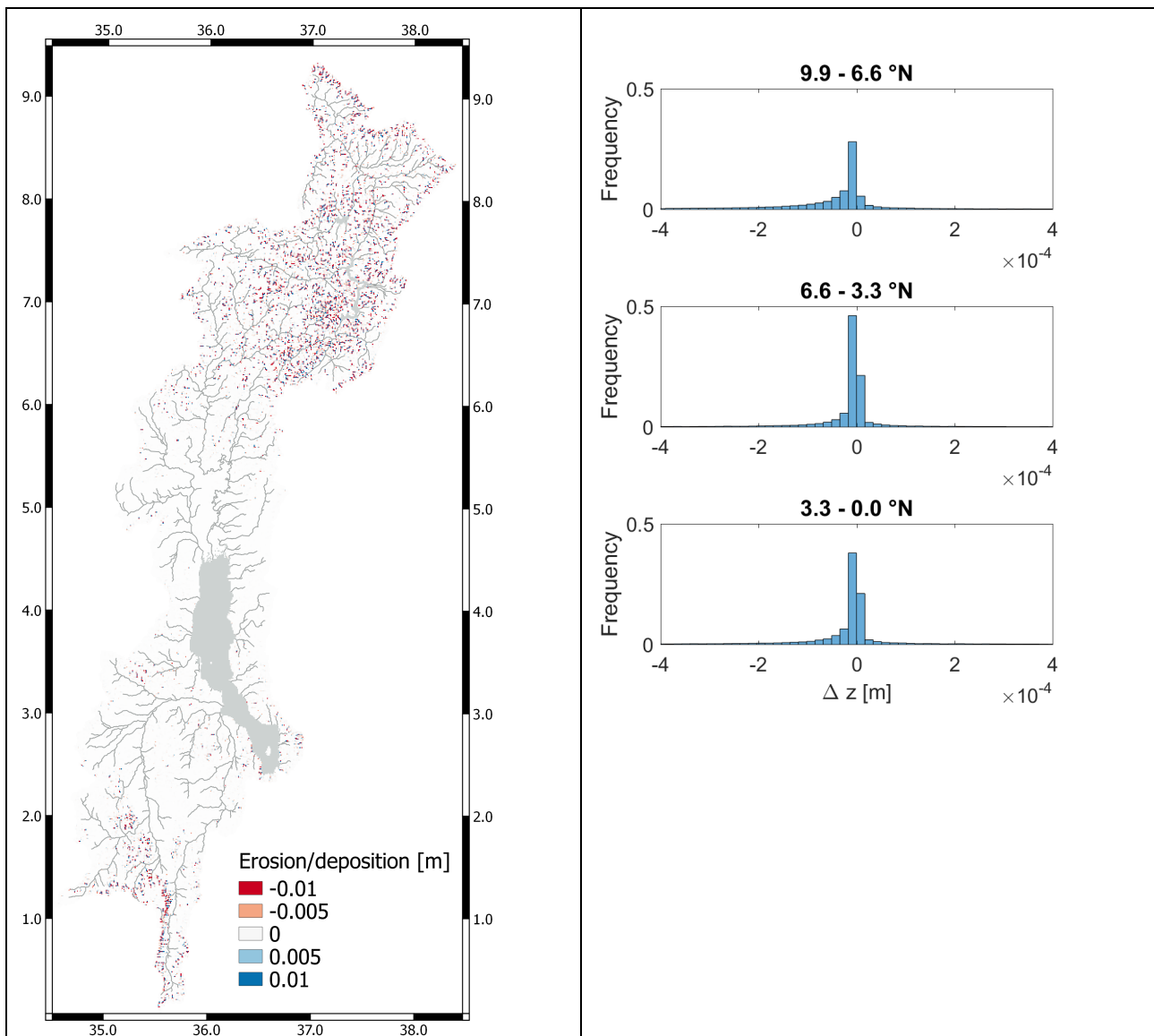


Figure A.3 – Erosion/deposition map simulated for the years 2016-2018 and frequency distribution of erosion and deposition values computed on single cells.

The mean daily sediment flux for the years 2016 to 2018 at the outlet of the main tributaries of Gibe I, Gibe III and Lake Turkana is reported in Figure A.4 for the two sediment trapping scenarios. Furthermore, also the sediment input into the Koysha reservoir has been monitored, even though the reservoir was not simulated. The total sediment load delivered by the river network to the reservoirs and the lake is shown in Table A.2 for the two trapping scenarios, together with their difference.

We observe that the sediment flux into Gibe I reservoir does not change between the two scenarios, as the soil erosion and sediment transport remain unaltered upstream of Gibe I. In Gibe III we observe a reduction of the peaks of the sediment flux, due to sediment retention in Gibe I. However, as shown by the annual sediment load, the effect of Gibe I is relatively small on the sediment input into Gibe III reservoir (12.5%). This is due to the high erosion taking place in the entire northern region of the Omo, which determines a high sediment supply from the tributaries joining the Omo downstream of Gibe I and from the Gojeb tributary (G\_III 2) which flows directly in Gibe III reservoir.

Sediment production on hillslope decreases rapidly in downstream direction of the Omo river, and it is minimum in the central region of the basin (Omo river floodplain). This reflects in the much big-



ger reduction of sediment flux at the stations K and T1 and of sediment load into the future Koysha reservoir and Lake Turkana. As mentioned above, Koysha reservoir is not modelled in the simulations, therefore the sediment flux and sediment load reduction at stations K and T1 are both determined by the Gibe I and Gibe III sediment retention. The high sediment supply from hillslopes in the northern part of the basin and the low sediment supply in the central region, imply that the more south the dams are located, the more they affect the sediment balance, because they disconnect the sediment production areas from the depositional areas.

Finally, it is notable that in the natural conditions (0% trapping scenario), the contribution of the tributaries Turkwel (T3) and Kerio (T4) is negligible compared to the sediment flux of the main Omo river. Instead, in the hypothesis of full sediment trapping in dams, the contributions of the two southern tributaries becomes comparable to the main Omo.

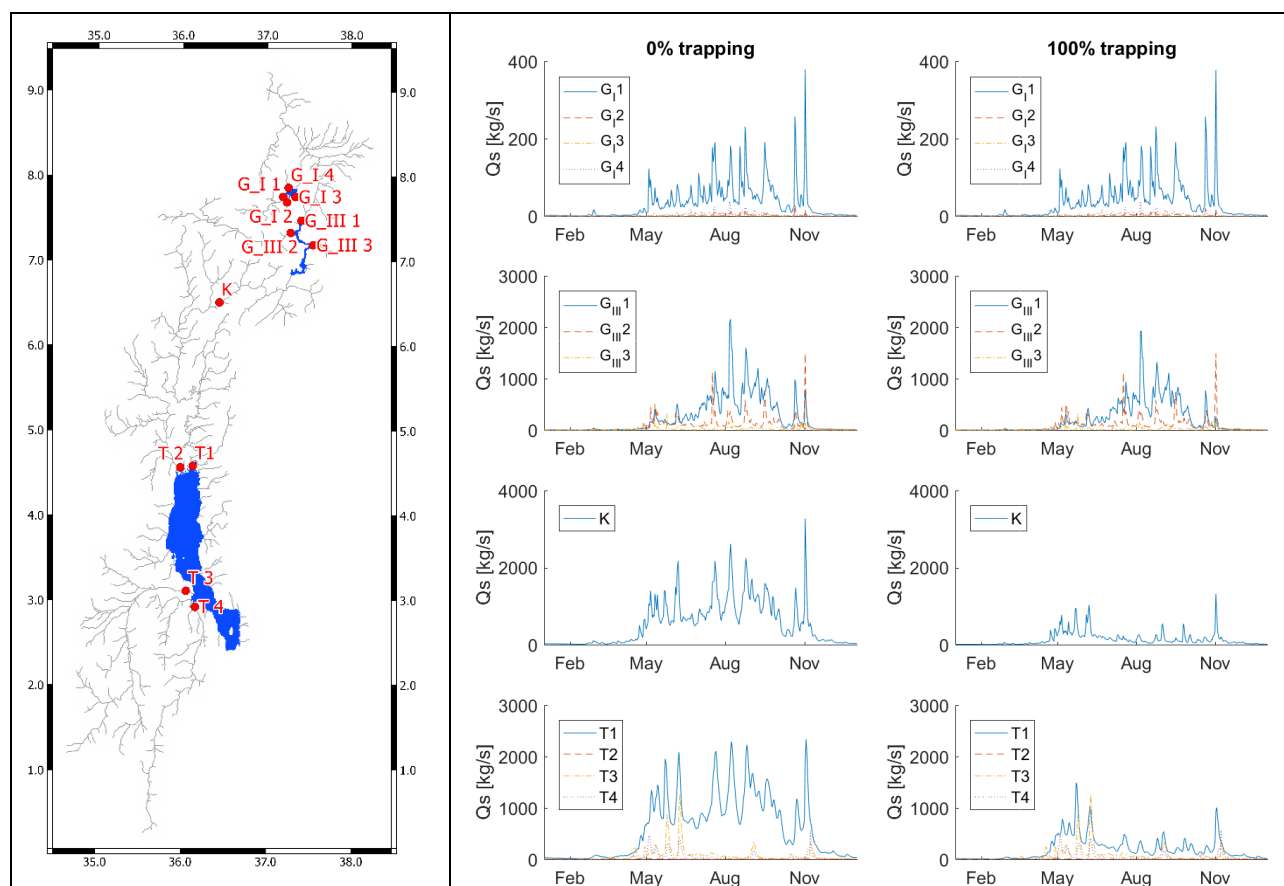


Figure A.4 – Mean sediment flux simulated for the years 2016-2018

Table A.2 – Measured vs modelled sediment load for two different trapping scenarios

	Mean annual sediment load [t]		Difference [%]
	0% sediment trapping	100% sediment trapping	
<b>Gibe I</b>	$1.17 \cdot 10^6$	$1.17 \cdot 10^6$	0.0
<b>Gibe III</b>	$10.94 \cdot 10^6$	$9.58 \cdot 10^6$	12.5
<b>Koysha</b>	$17.19 \cdot 10^6$	$4.14 \cdot 10^6$	75.8
<b>Lake Turkana</b>	$22.60 \cdot 10^6$	$9.65 \cdot 10^6$	57.3